A NEW APPROACH TO ASSESS ARTERIAL SYSTEM FUNCTION

WITH COMPLIANCE-PRESSURE LOOP

By

YUEYA GE

A thesis submitted to the

School of Graduate Studies

Rutgers, The State University of New Jersey

In partial fulfillment of the requirements

For the degree of

Master of Science

Graduate Program in Biomedical Engineering

Written under the direction of

Professor John K-J. Li

And approved by

_____

_____

_____

New Brunswick, New Jersey

October 2018

ABSTRACT OF THE THESIS

A New Approach to Assess Arterial System Function

with Compliance-Pressure Loop

by YUEYA GE

Thesis Director:

Professor John K-J. Li

High blood pressure has been recognized as a most common risk factor of cardiovascular diseases, which is the leading cause of death. There is a strong correlation of blood pressure(P) and mechanical properties of arteries, as characterized by vascular compliance, peripheral resistance and characteristic impedance. For this reason, an accurate estimation of these parameters is necessary for better interpretation of arterial system function and hypertension.

The classic Windkessel model is one of the most popular tools in the clinical setting to describe arterial system function. This model assumes a constant arterial compliance(C) throughout the entire cardiac cycle, although it has been known that compliance is a function of pressure. A recently modified Windkessel, also known as Li

model, which incorporates a pressure-dependent nonlinear compliance(C(P)) component has shown that arterial compliance is varying along time, i.e. not a constant value.

In this thesis, simultaneously measured aortic pressure and flow data were gathered during normal, hypertension and vasodilator conditions. The accuracy of the nonlinear C(P) model predicted waveforms is first established. This is followed by the use of a new compliance-pressure loop (CPL) approach to evaluate arterial system function under varied vasoactive conditions over a wide range of pressure. Results show CPL can provide a rapid visualization of arterial system function and that reduced compliance due to hypertension and improved compliance due to vasodilator can be readily quantified. This CPL method thus can be further applied to the assessment of severity of hypertension and clinical assessment of drug efficacy.

Acknowledgements

First, I would like to thank my advisor, Dr. John K-J. Li, for his guidance and patience. I obtained great amount of research experience and good opportunities for on-site training working with Dr. Li, who also encourages me that never forget to enjoy my life.

I would also thank my family for always being loving and supportive to me. Without their love and company, I would not have enough courage and confidence to chase my dream and focus on my school work.

In this thesis, the existing data was from historical animal experiments that Dr. Li conducted in his previous research. Also, part of this project has been published in Computers in Biology and Medicine (CBM), where I was included as a co-author that contributed my master's research work including codes, methods and figures to this journal paper.

Table of Contents

List of Tables

List of Illustrations

Chapter 1. Introduction

1.1 Blood Pressure and Hypertension

The human heart is the source of pulsatile pressure and flow generation. Blood pressure usually refers to the pressure generated by the flowing blood against the vessel walls. It is mainly associated with blood volume and the properties of vessel walls. It is also determined by the cardiac output, peripheral resistance and arterial compliance from the view of hemodynamics. A normal resting blood pressure for adults is approximately 120/80 mmHg for systole/diastole, as defined by the American Heart Association (AHA). People with readings of over this standard will be considered as having hypertension, i.e. 140/90 mmHg.

Hypertension is one of the most prevalent diseases and the leading cause of death in United States as well as to the world as a whole. Additionally, its prevalence does not appear in decline trend over 4 decades even though the technology of diagnosis and the treatment for hypertension has been improving rapidly (Kannel,1996). Among all the risk factors of cardiovascular disease, hypertension continues attracting attentions from clinicians and researchers because of its dominant effect on causing a heart failure.

In November 2017, American Heart Association (AHA) redefined the readings of potential hypertension conditions as 130/90 mmHg, this modification resulted in 14 percent increase in U.S. adults that are identified with a high blood pressure, from 32 percent previously to 46 percent now under the new definition (AHA,2017).

1.2 Blood Pressure Measurement

The traditional blood pressure measurement is using a mercury sphygmomanometer. This is also known as the cuff method by which a cuff is placed smoothly around an upper arm in a hospital setting, to record the systolic pressure and diastolic pressure. They are detected by the appearance and disappearance of the two "Korotkoff" sounds (thus "auscultatory"), respectively. Although this technique has been in a long run regarded as a "gold standard" for blood pressure measurement, its high association with patient status, hospital settings brings a source of error that gradually diminishes its role in clinical practice. Besides the lack of accuracy, continually varying in blood pressure makes auscultatory method cumbersome. It has slowly phased out over time due to an inadequate description by only two numbers (Pickering, 2006). As pressure changes throughout the entire body, monitoring of pressure waveform becomes more necessary in order to have a better understanding of arterial properties, for more accurate diagnosis and improve the treatment of hypertension.

As early as in 1973, photo-plethysmograph (PPG) technique was first introduced by Penaz (Penaz, 1973.), a small cuff was placed on fingers to detect arterial pulsation. Because the output of PPG remains constant to drive a servo-loop, any change in the cuff pressure caused by pressure pulse at fingertip would be counteracted and pressure waveforms for each cardiac cycle can be completely recorded then be digitized through computation. This scheme is non-invasive, can be implemented without limit on subject's postures or positions and gives an accurate estimate in pressure varying from systole to diastole compared to branchial artery pressures (Ogedegbe et al., 2010). Similar non-invasive measurements emerged in recent years include ultrasound techniques, artery

tonometry. However, the aortic pressure, which is exerted on the heart and brain, was acknowledged to be different from the pressure measured at the arm (Agabiti-Rosei et al., 2007). Therefore, for further analysis of central blood pressure, invasive methods are employed as those non-invasive ways can only directly estimate peripheral arterial pressure.

Catheterization, an invasive technique, is the most common procedure in current clinical use of evaluating central blood pressure. With tiny semiconductor pressure sensors, the so-called catheter-tip pressure transducers, attached along the plastic tube, and inserted through the femoral artery, central aortic pressure can be accurately measured. Pressure signals are then recorded and digitized by a computer for further analysis. The rationale behind this process is that central blood pressure has been identified as more relevant for pathogenesis of cardiovascular diseases compared to peripheral pressure as the latter is largely affected by acceleration of wave reflections especially at branching sites (Nichols et al., 2005; Safar et al., 2006).

1.3 Arterial Compliance

Contraction of the heart is a pulsatile activity that pumps blood into aorta. Ventricular outflow differs in each person and is primarily associated with the properties of aorta. Both aging and hypertension exist with arterial load changes. Vascular load is represented by changes in arterial compliance and peripheral resistance. Additionally, inertance due to blood mass and flow acceleration, eventually causes the acceleration in arterial structural change.

In past decades, arterial stiffness has been recognized as a crucial determinant of cardiovascular morbidity (Laurent et al., 2001; Vlachopoulos et al., 2010; Mitchell et al.,

2010; Safar, 2001) because it is considered as tightly relating to hypertension, higher risk of atherosclerosis and many other conditions that potentially augment heart failure. In order to evaluate wall stiffness in hypertension diagnosis, arterial compliance has become a significant index. Its reduction suggests an increased or greater stiffness of arteries.

Mathematically, arterial compliance is defined as the volume change of blood flow divided by simultaneously pressure difference:

$$\mathrm{C} = \frac{dV}{dP} \tag{1.1}$$

1.4 The Windkessel Model: The Lumped Model of the Arterial System

The concept of Windkessel was originally conceived by the English clergyman Stephen Hales in 1733 to mimic the action of the fire hoses, as he called it air-chambers. Windkessel is the German word of air-bellow, following the use by Otto Frank a century later. The air chamber or the reservoir, was taken to imply a volume elasticity of large arteries as these arteries distend during systole in consist with higher blood pressure while on elastic recoil during diastole with low blood pressure to help damp the fluctuation in blood pressure. Also, it is Otto Frank who quantitatively formulated the lumped Windkessel model, incorporating a resistance and a compliance element. (Frank, 1990). Because the interaction and coupling between the heart and the arterial system is complicated, the lumped Windkessel model is a fairly accurate tool for simplification and understanding the function of entire arterial circulation.

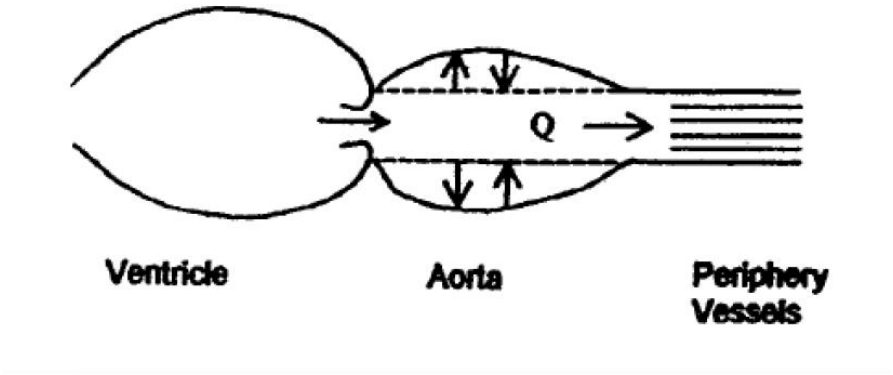

Fig 1.1: Coupling of the left ventricle (LV) and arterial system based on Windkessel concept. (Li, 2004, with approval).

In the electrical representation of the first-developed 2-element Windkessel model (Fig 1.2), a resistor (Rs) characterizes the peripheral resistance of arteries to blood flow for its viscous properties, while a capacitor (C) is used to illustrate arterial compliance which has storage properties. Frank's goal was to obtain stroke volume from measured pressure pulse contour and it did predict that during diastole, the pressure decays exponentially with a characteristic time constant.

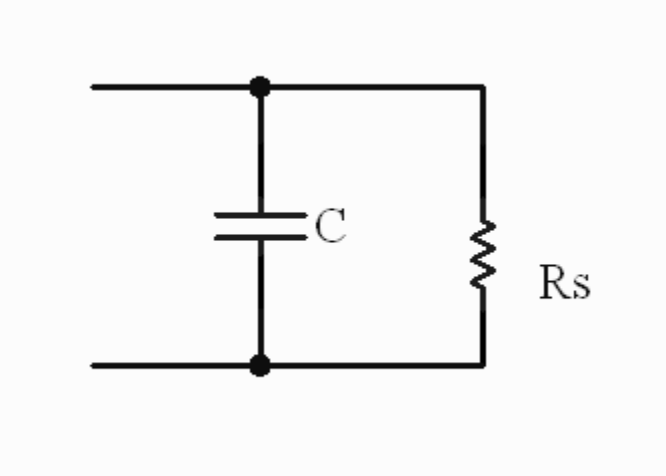

Fig 1.2: The electrical analog model of the two-element Windkessel model in which C=arterial compliance, Rs=peripheral resistance.

Although two-element Windkessel model gives a good prediction on pressure decay during diastole, it is inadequate to depict the relation between pressure and flow during systole. Three-element model (Fig 1.3) was then developed by adding an aortic characteristic impedance element to the classical two-element model, which is still widely utilized in researches today. In the three-element model, one resistor (Zo) is added in series on previous model to represent the characteristic impedance which acts analogically to a resistor in circuit. Characteristic impedance can be defined in time domain as the ratio of oscillatory pressure to blood flow at the entrance of aorta under the condition that no reflected waves reach to this input, it is a crucial determinant of the left-ventricular load during ejection (Dujardin et al., 1981).

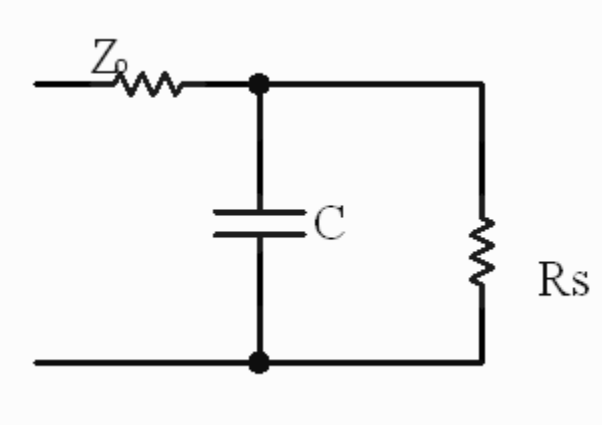

Fig 1.3: Electrical analog model of the three-element Windkessel model. Arterial compliance, peripheral resistance and characteristic impedance are represented by a capacitor, a resistor and a resistor, respectively. Zo=characteristic impedance, Rs= peripheral resistance, C=arterial compliance.

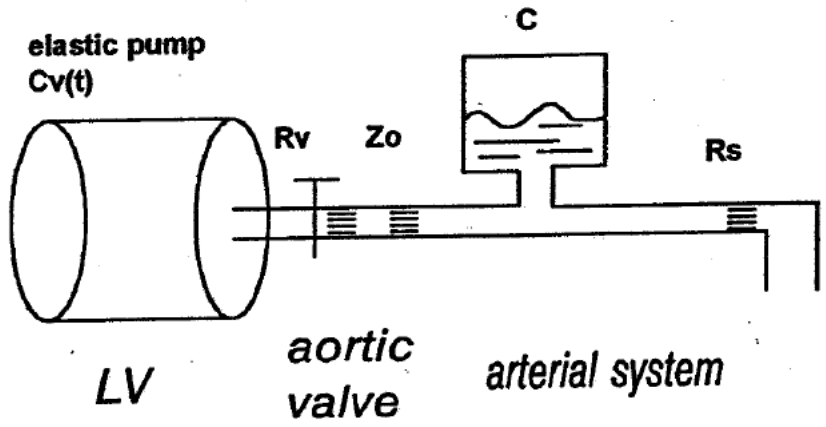

Fig 1.4: The hydraulic equivalent of the three-element Windkessel model. Arterial compliance is represented by a bottle where the volume varies with pressure change. A needle valve is used to illustrate the change of peripheral resistance to blood flow while the characteristic impedance of the aorta is symbolized as a finite tube (Li, 2004, with approval).

1.5 Pulse Wave Reflections

Study of input impedance(Z) of the aorta, which is defined as the harmonic ratio of pressure oscillation to flow oscillation, laid the groundwork for identifying properties of the arterial system. With the knowledge of the characteristic aortic impedance Zo (which has no dependence on wave reflection), forward and backward traveling pulse waves can be separated. Structural and geometric nonuniformities could be identified for causing the wave reflections on pressure and flow waveform while they are propagated through the vascular tree. It should be noted here that reflected pressure and flow waveforms are 180° out of phase (Li, 2004). Namely, increase in wave reflection amplitude will lead to augmentation in pressure and decrease in blood flow.

$$\mathrm{Zo} = \frac{P_f}{Q_f} \tag{1.2}$$

Any measured blood pressure and flow can be resolved into forward and reflected flow:

$$\mathrm{P} = \mathrm{P}_f + \mathrm{P}_r \tag{1.3}$$

$$\mathrm{Q} = \mathrm{Q}_f + \mathrm{Q}_f \tag{1.4}$$

And these components can be obtained if we calculate out the characteristic impedance Zo:

$$\mathrm{P}_f = \frac{(\mathrm{P}+\mathrm{QZo})}{2} \tag{1.5}$$

$$\mathrm{P}_r = \frac{(\mathrm{P}-\mathrm{QZo})}{2} \tag{1.6}$$

P: measured pressure

Q: measured flow

P_f: forward pressure

P_r: reflected pressure

Z: characteristic impedance

While the basic foundations of hemodynamics have been laid, the understanding of the interdependence of arterial compliance, wave reflections and blood pressure amplitudes are still unclear.

Chapter 2. Aims and Significance of the Thesis

2.1 objective of the Thesis

Computational tool for prediction of aortic pressure and flow has marked value in describing arterial functions. The Windkessel model, as a most popular schema, has been involved into numerous studies, assisting in estimation of mechanical properties of arteries. Nonetheless, a modified Windkessel model consisting the pressure-dependent compliance component in this study can improve the prediction outcome. Furthermore, a novel concept of compliance-pressure loop representatively indicates the quantitatively change in vessel wall properties.

2.2 Specific Aims

This thesis focuses on:

1. Utilizing a modified three-element Windkessel model with pressure-dependent compliance.

The classical two-element and three-element Windkessel model demonstrates the arterial compliance as functioning as a capacitor with a constant capacity, in other words, predictions based on these assumptions will define a linear relationship between blood flow and the rate of change of pressure. In reality, vascular channels are inherently nonlinear, however, linear modellings neglect the interaction between blood pressure and arterial compliance (Liu et al., 1989; Wang et al., 2006). To better approximate the outflow with pressure dependence of the arterial compliance being considered, a non-linear three-element Windkessel model was proposed, in which a pressure-dependent compliance element (C(P)) replaces constant compliance (C) (Li et al., 1990).

2. Introduce a new approach with the compliance – pressure loop (CPL)

Despite that multiple indices have been proposed to evaluate the arterial stiffness such as cardio-ankle vascular index (Shirai et al., 2006), pulse wave velocity (PWV), elastic modulus, a more recent concept of pressure-compliance loop is introduced in this thesis. This concept is based on the fact that compliance is varying continuously throughout the cardiac cycle and reveals the characteristic of compliance in systole or in diastole.

3. Forward and reflected pressure derived from nonlinear modelling

In this thesis, antegrade and retrograde components of predicted central pressure were computed under a control and a hypertensive condition. The wave reflections were analyzed combined with the arterial compliance for each case.

2.3 Significance of the Thesis:

Over the years, cardiovascular disease (CVD) has been indicated as having fatal impact to human lives. In 2015, heart disease led to 633,842 deaths in United States, ranking the top among causes of death (Murphy et al., 2015). Moreover, 28.1 million adults in United States were diagnosed as having heart disease in 2016, which takes up 10.7% of total population, also in which the hypertension accounts for the largest proportion as of 24.9% (Summary Health Statistics: National Health Interview Survey, 2016).

Efforts have been devoted to achieving in advanced technology of diagnosing and curing CVD due to its serious effect. More recently, computational tools are commonly

involved in clinical research, contributing to developing new method and perspectives in treatment.

With the cardiovascular diseases especially as hypertension still being the main cause of global mortality, improvement in diagnostics, treatment and monitoring would greatly benefit the current clinical practice. A better understanding of hemodynamics and mechanical properties of vessels will allow physicians to treat patient more properly, hopefully, to prevent those diseases from occurring. Developing a model-based analytical system can help determining vascular conditions more accurate, more efficient and less invasive to patient. Furthermore, this technology can be used in evaluating the effect of medicines, helping patients and clinicians to recognize the best vasodilator treatment in caring for heart failures.

Chapter 3. Methods

3.1 Animal Data Collection

Experimental data is collected from previous experiments performed on anesthetized, ventilated mongrel dogs with approval of the Rutgers University Institutional Animal Care and Use Committee (IACUC) (Segers et al. 1999; Li et al., 1994; Kaya et al., 2018). An electromagnetic flow probe was placed at the ascending aorta to measure aortic blood flow. Simultaneously, a Millar catheter-tip pressure transducer was inserted from the femoral artery to record the aortic pressure. Vasodilation and vasoconstriction were induced with intravenous bolus infusion of nitroprusside (50 μg/ml) and methoxamine (2-5 mg/ml), respectively. Aortic pressure and aortic flow were thereafter recorded at steady state under the normal(control), hypertension (vasoconstriction) and subsequent hypotension (vasodilation) conditions. Lead II electrocardiogram was utilized to monitor the heart condition. Collected data were then sampled at a frequency of 100 Hz for later computations. In this study, we selected 5 datasets of control, 3 datasets of hypertension and 3 for hypotension as they spread a wide pressure range that we could have a comprehensive view of varied vessel wall property conditions. This allows pressure-dependence characteristics of arterial compliance to be examined closely.

3.2 The Nonlinear three-element Windkessel Model:

A modified three-element Windkessel model incorporating a pressure dependent compliance(C(P)) element was represented by the analog diagram shown in Fig 3.1. Instead of a constant capacitor, a variable capacitor was used to symbolize C(P).

Furthermore, C(P) in this model was expressed as an exponential function of the peripheral pressure, i.e.

$$C(P) = a * e^{b(P(t))} \tag{3.1}$$

This expression was first proposed in 1990 (Li et al., 1990), and is known as the Li model. Here, a and b are empirical constants. The mutual effect between arterial stiffness and arterial pressure is well demonstrated in this equation.

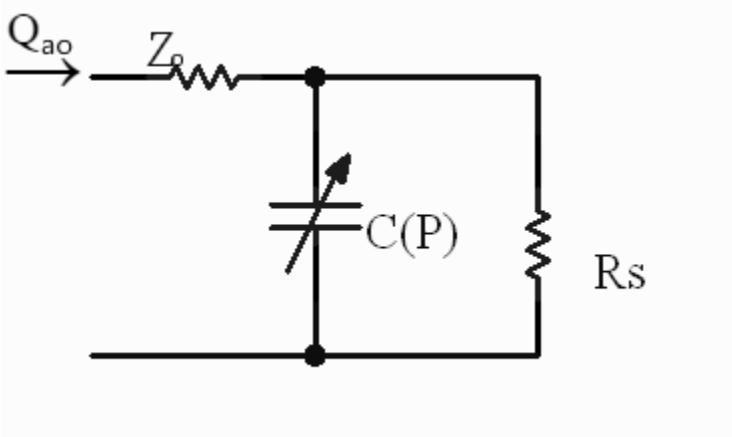

Fig 3.1: The modified Windkessel model (the Li model). The model consists of a pressure dependent compliance element (C(P)), the peripheral resistance (Rs) and the characteristic impedance of the proximal aorta (Zo). Qao, the aortic flow is considered as the input of this model (Li et al., 1990).

3.3 Parameter Estimation of the Nonlinear Model:

Peripheral resistance (Rs) is calculated by the ratio of mean aortic pressure and mean aortic flow, representing the steady load to the heart:

$$R_s = \frac{\overline{P_{ao}}}{\overline{Q_0}} \tag{3.2}$$

In time domain, characteristic impedance Zo can be approximated by the instantaneous ratio of change in pressure and flow, where change in pressure is defined as from end-diastolic pressure to certain pressure in the first 60-80 ms of ejection. This approximation is based on the fact that during early ejection, the backward flow from the periphery have not appreciably reached the proximate aorta, therefore Zo can be obtained from instantaneous pressure change and flow (Li, 1986).

$$Z_o = \frac{P(t) - P_{ed}}{Q(t)} \tag{3.3}$$

In our cases, we utilized data of pressure and flow from first 50 ms of ejection to mostly avoid the effect from reflected waves, taking the specific condition of subjects into consideration as well. Moreover, an average of Zo was calculated in our analysis to reduce errors.

The aortic flow, also known as total inflow to the vascular system, is a summation of flow stored during heart contractions and flow that goes to small peripheral vessels. The storage property of vessels can be described by compliance, which is also illustrated by the change in blood volume due to a change in distending pressure. The amount of stored flow can be therefore expressed as a product of compliance and rate of change in pressure.

$$Q_i = Q_s + Q_o \tag{3.4}$$

$$Q_s = \mathrm{C} \cdot \frac{dP}{dt} \tag{3.5}$$

Substituting this equation with (3.4).

A total flow consisting of a pulsatile component and a steady component can be mathematically described with Windkessel parameters C and Rs.

$$\mathrm{Q} = \mathrm{C} \cdot \frac{dP}{dt} + \frac{\mathrm{P}}{R_s} \tag{3.6}$$

During diastole, the heart distends, and no blood flow pumped into the aorta, in other words, the inflow is zero (equation 3.6 equals 0).

$$\mathrm{Q} = \mathrm{C} \cdot \frac{dP}{dt} + \frac{\mathrm{P}}{R_s} = 0$$

Or

$$\frac{dP}{P} = -\frac{dt}{R_s C} \tag{3.7}$$

Integrating both sides of equation (3.7) gives us

$$\mathrm{P} = P_o \, e^{\frac{-t}{R_s C}} \tag{3.8}$$

As this equation indicates that diastolic aortic pressure relies on both peripheral resistance and compliance, a time constant of pressure decay τ is then determined as product of these two components:

$$\tau = R_s C \tag{3.9}$$

Equation (3.8) can be recast:

$$\mathrm{P} = P_o \, e^{\frac{-t}{\tau}} \tag{3.10}$$

Specifically, we substitute P with end-diastolic pressure Pd and substitute Po with end-systolic pressure Pes as they are easy to be identified in pressure waveforms (Fig 3.2).

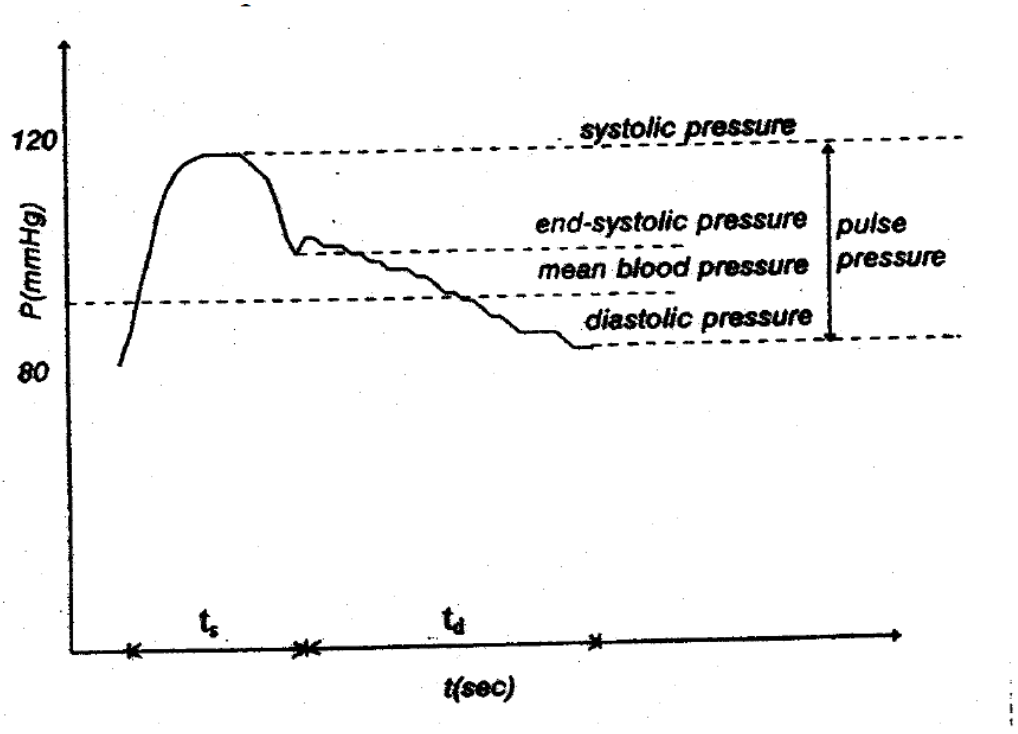

Fig 3.2: Illustration of a typical aortic pressure waveform in a single cardiac cycle. The systolic pressure, end-systolic pressure, mean blood pressure, diastolic pressure and pulse pressure are all marked. The time duration of one contraction is separated into systolic time and diastolic time (Li, 2004, with approval).

Transforming equation (9) and (10) finds us a way to calculate constant compliance C and time constant τ.

$$C = \frac{t_d}{R_s ln\frac{P_{es}}{P_d}} \tag{3.11}$$

$$\tau = \frac{t_d}{ln\frac{P_{es}}{P_d}} \tag{3.12}$$

However, equation (3.11) is only valid for constant compliance. When we apply a pressure-dependent compliance C(P) (3.1) to the system, the computation will be more complicated:

$$Q_c(t) = Q(t) - \frac{P(t)}{R_s} \tag{3.13}$$

Where Qc(t) represents the flow stored in vessels that has an alternative equation based on circuit theory:

$$Q_c(t) = C(P) \cdot \frac{dP(t)}{dt} \tag{3.14}$$

Combination of equation (13) and (14) results in

$$\frac{dP}{dt} = \frac{Q(t) - \frac{P(t)}{R_s}}{C(P)} \tag{3.15}$$

The rate of change in pressure is associated with flow, peripheral resistance and a nonlinear compliance.

From the definition of time increment:

$$\Delta t = t_{i+1} - t_i = dt \tag{3.16}$$

Where dt, in this case, is the sampling interval of 10msec.

Pressure can be obtained point by point in a time manner

$$P(t_{i+1}) = P(t_i) + \Delta t \cdot (Q(t_i) - (P(t_i))/Rs\ )/(C(P)) \tag{3.17}$$

Eventually, the aortic pressure $P_a(t)$ will be predicted by the numerical procedure using measured flow, characteristic impedance and simulated peripheral pressure

$$P_a(t_i) = Q(t_i) \cdot Z_o + P(t_i) \tag{3.18}$$

Algorithm was developed and programmed with MATLAB to estimate parameters ‘a’ and ‘b’ following steps below:

Step 1: Prepare peripheral resistance Rs and characteristic impedance Zo with given pressure and flow data.

Step 2: Initialized parameter ‘a’ to 0.1, ‘b’ to -0.6, and put them into loops with increment of 0.1 and 0.01, respectively. Peripheral pressure P(t) was initialized to the end diastolic pressure or first value of aortic pressure.

Step 3: C(P) was determined with assigned ‘a’ and ‘b’ pair and was involved in generating peripheral pressure waveform.

Step 4: Aortic pressure was predicted with estimated characteristic impedance and its corresponding flow.

Step 5: For each pair of ‘a’ and ‘b’, the root mean square error (RMSE) between predicted aortic pressure and the measured one was computed and saved for later comparison.

$$RMSE = \sqrt{\frac{1}{N}\sum_{i=1}^{N}\left(P_a^{estimated}(t_i) - P_a^{measured}(t_i)\right)^2} \tag{19}$$

Where N is the amount of data points.

Step 6: After repeating the entire process with all possible pairing of ‘a’ and ‘b’, where ‘a’ ends up at 6 and ‘b’ ends up at -0.01, their RMSEs were compared. Optimal ‘a’ and ‘b’ value were decided which have the minimum RMSE.

In order to illustrate the advantage of nonlinear Windkessel model, linear Windkessel model derived constant compliance (C from equation 3.11) and ratio of stroke volume and pulse pressure method (C_v) were also employed to derive the compliance and following predictions:

$$C_v = \frac{SV}{PP} \tag{3.20}$$

Stroke volume SV was calculated as the product of mean blood flow and duration of one cardiac cycle and the pulse pressure PP is basically the difference between the systolic pressure and the diastolic pressure.

$$\mathrm{SV} = \bar{Q} \cdot t \tag{3.21}$$

Chapter 4. Results

4.1 Predictions on aortic pressure with linear and nonlinear Windkessel Model

The merit of the nonlinear pressure-dependent compliance model, or the Li model, is compared with the classic Windkessel model. This is most clearly illustrated from the comparison of computed pressure waveforms with the experimentally measured waveforms. Results are shown for all processed data.

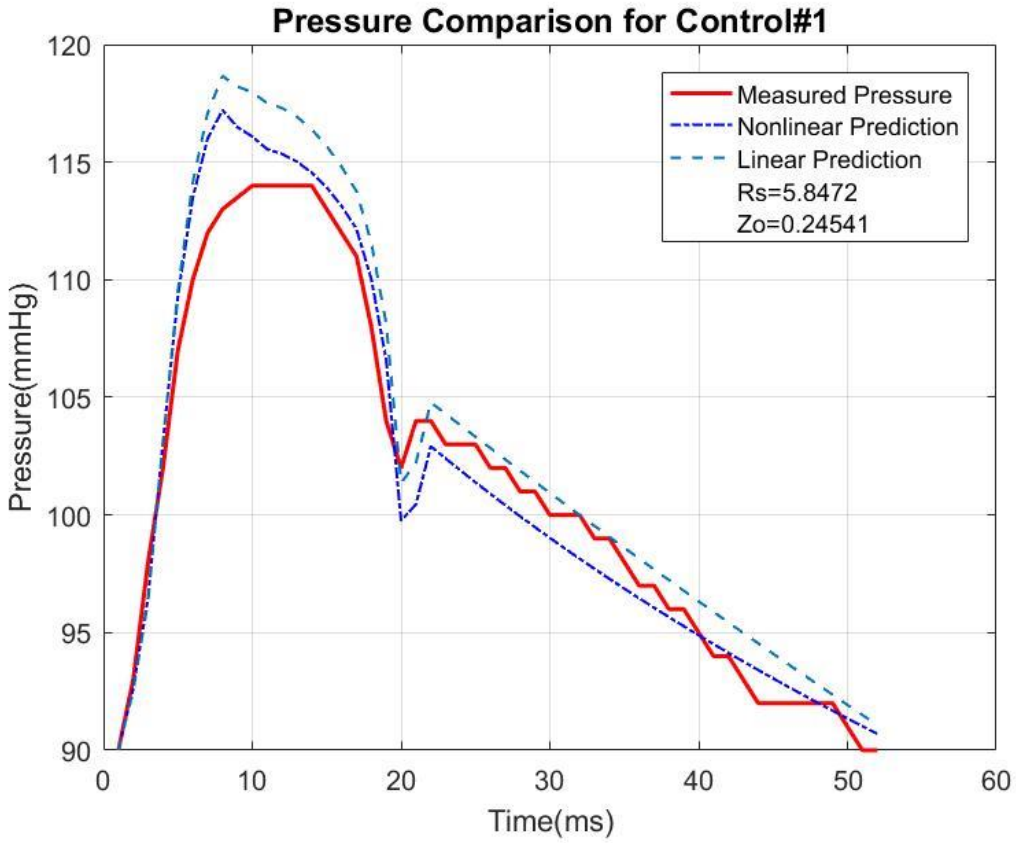

Fig 4.1: Aortic pressure approximation for control #1. Pressure of normal case #1 predicted by linear Windkessel model, nonlinear Windkessel model, compared with measured aortic pressure.

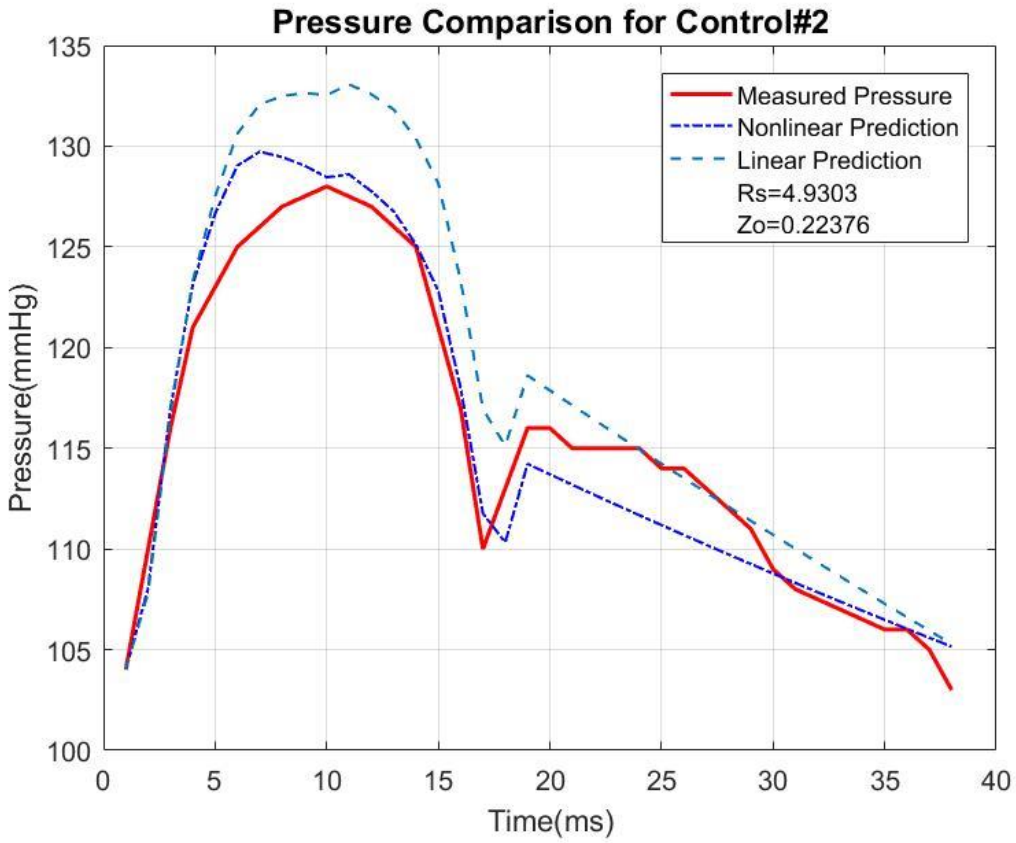

Fig 4.2: Aortic pressure approximation for control #2. Pressure of normal case #2 predicted by linear Windkessel model, nonlinear Windkessel model, compared with measured aortic pressure.

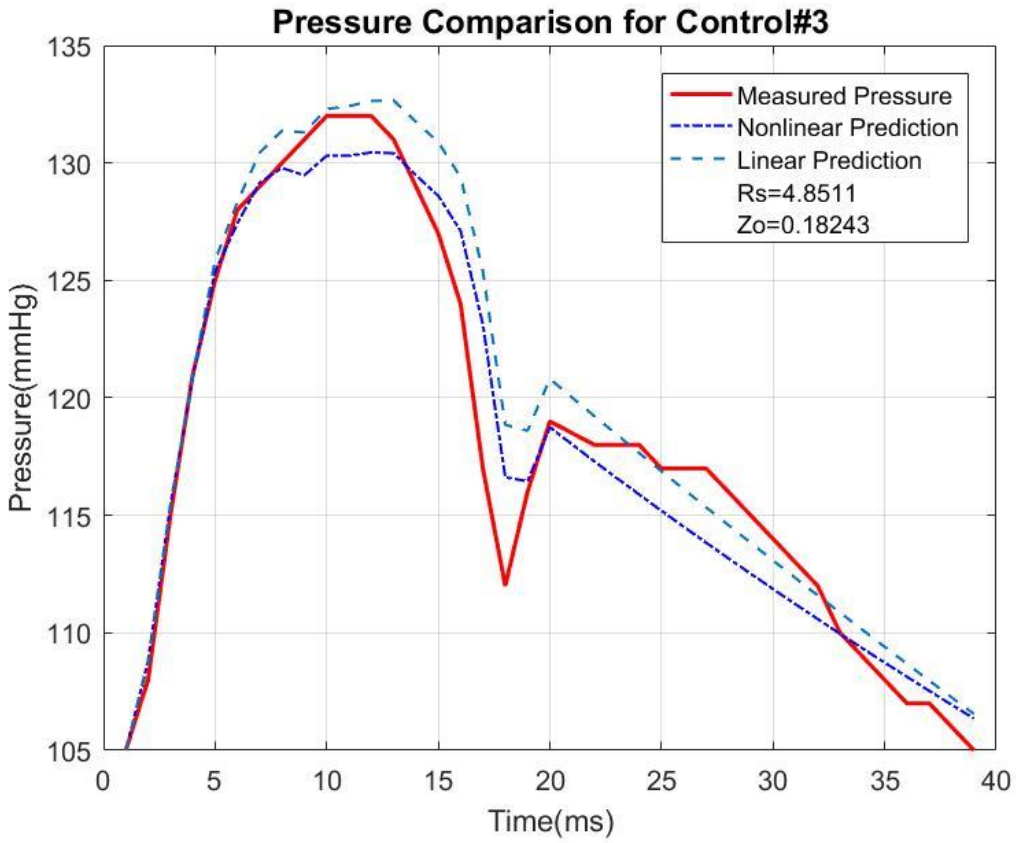

Fig 4.3: Aortic pressure approximation for control #3. Pressure of normal case #3 predicted by linear Windkessel model, nonlinear Windkessel model, compared with measured aortic pressure.

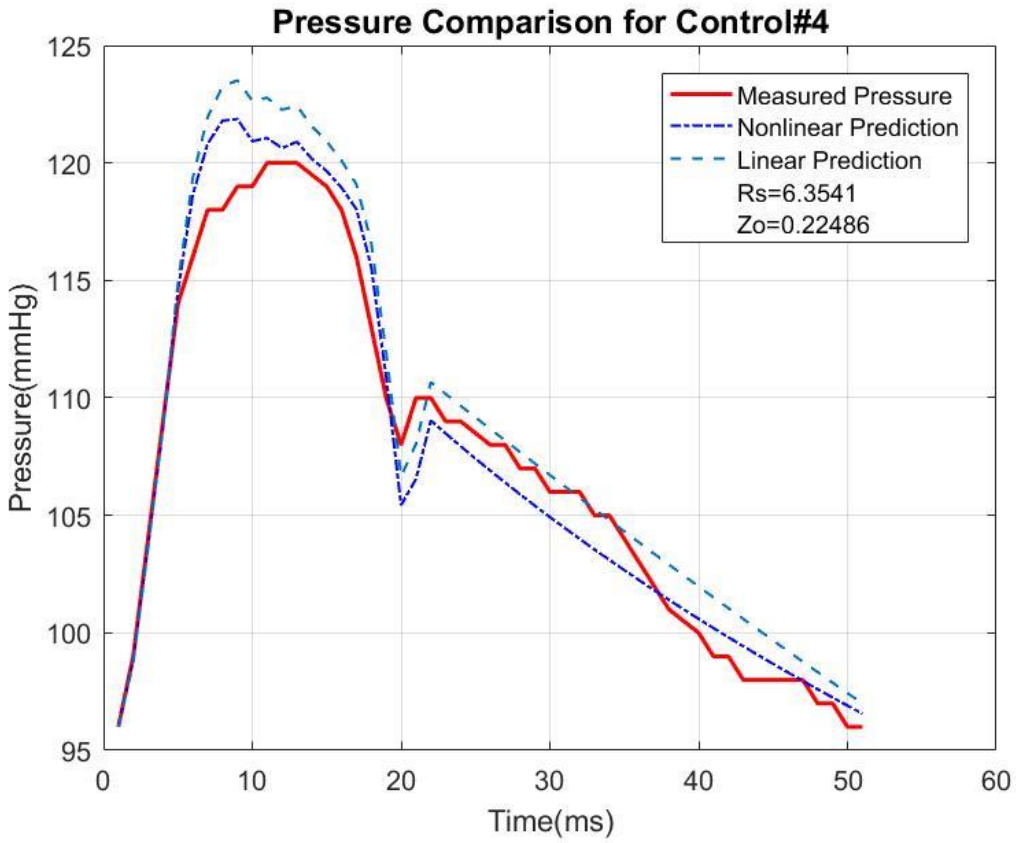

Fig 4.4: Aortic pressure approximation for control #4. Pressure of normal case #4 predicted by linear Windkessel model, nonlinear Windkessel model, compared with measured aortic pressure.

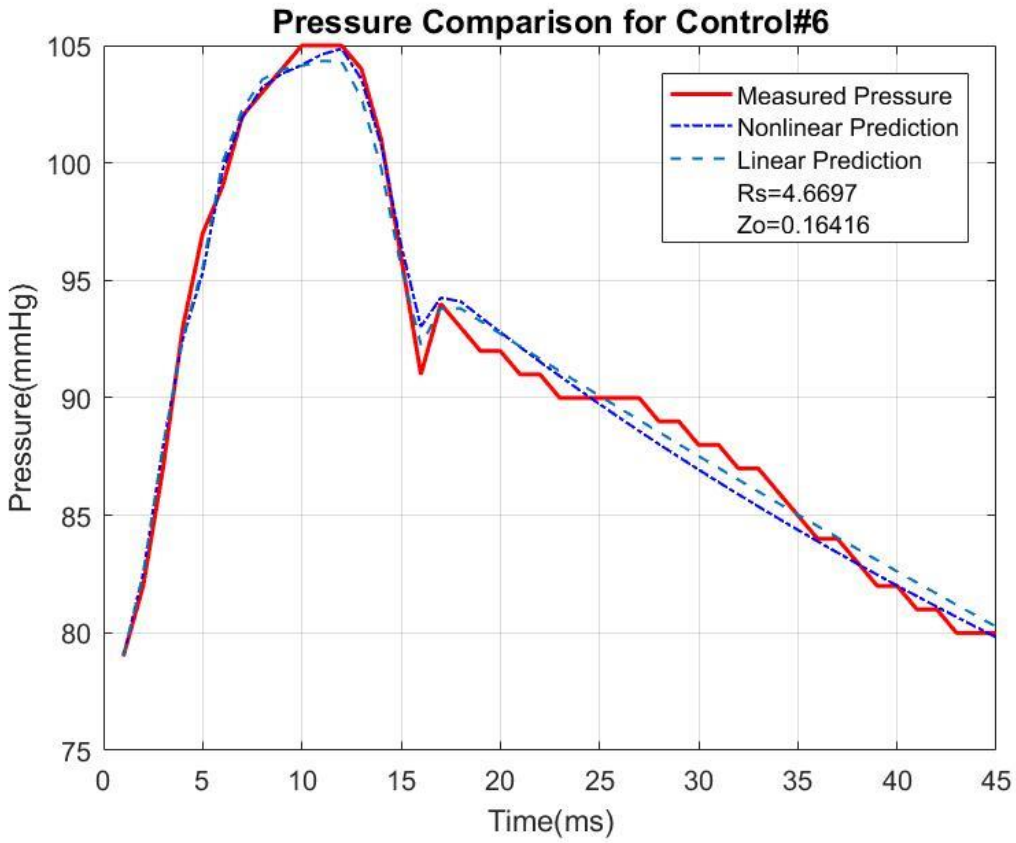

Fig 4.5: Aortic pressure approximation for control #6. Pressure of normal case #6 predicted by linear Windkessel model, nonlinear Windkessel model, compared with measured aortic pressure.

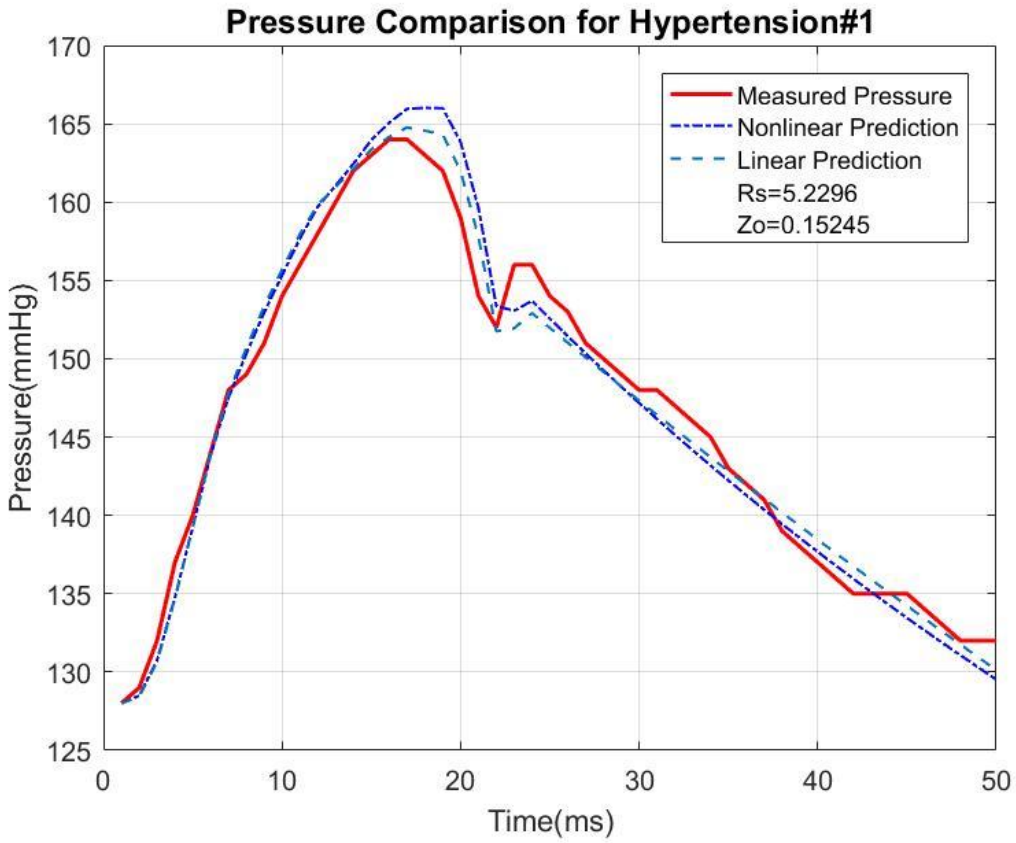

Fig 4.6: Aortic pressure approximation for vasoconstriction #1. Pressure of hypertension case #1 predicted by linear Windkessel model, nonlinear Windkessel model, compared with measured aortic pressure.

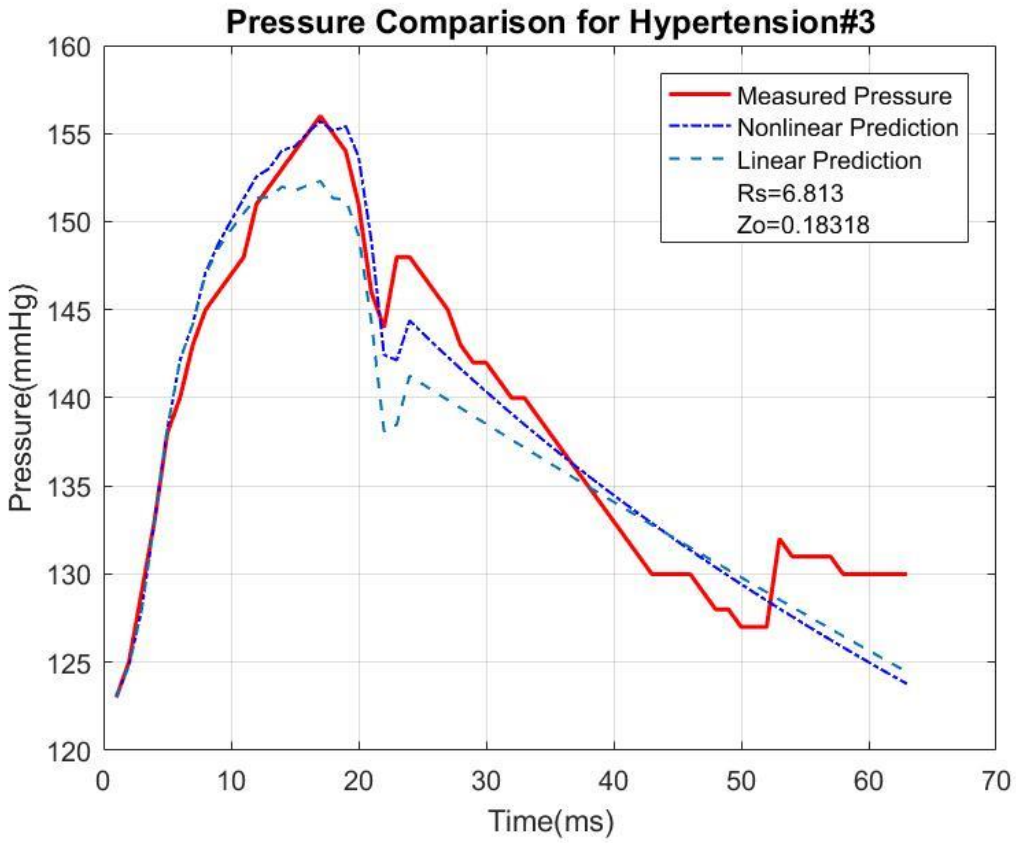

Fig 4.7: Aortic pressure approximation for vasoconstriction #3. Pressure of hypertension case #3 predicted by linear Windkessel model, nonlinear Windkessel model, compared with measured aortic pressure.

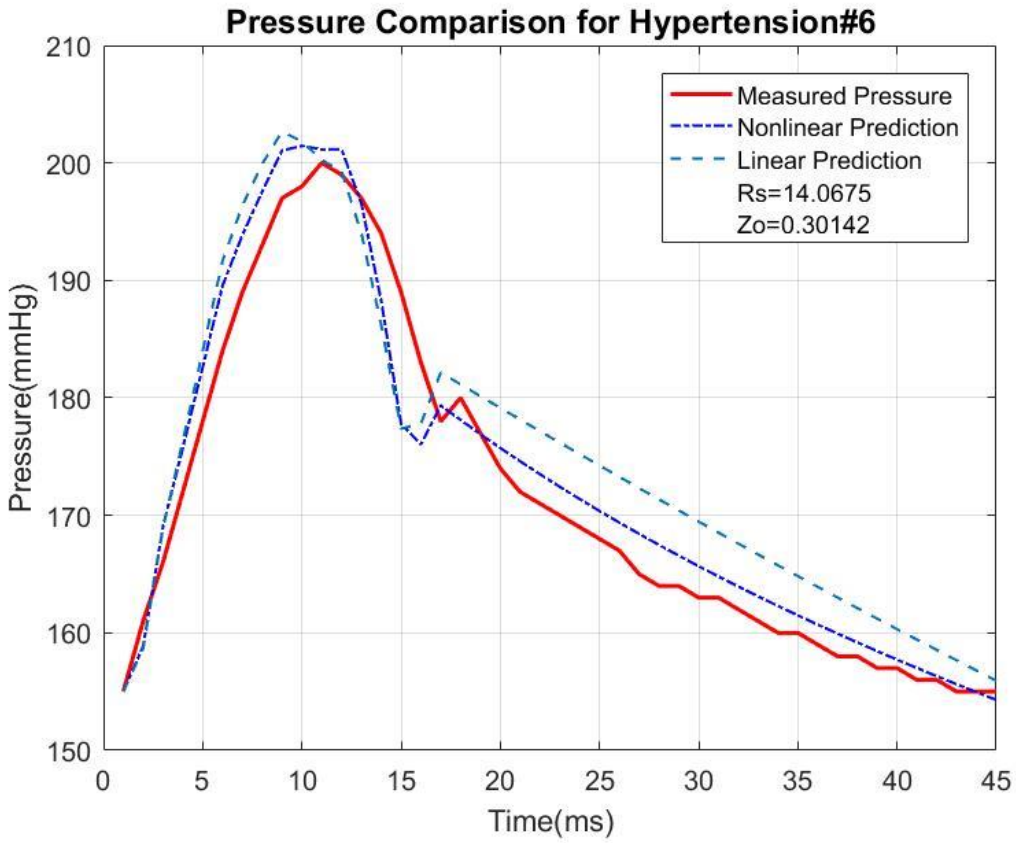

Fig 4.8: Aortic pressure approximation for vasoconstriction #6. Pressure of hypertension case #6 predicted by linear Windkessel model, nonlinear Windkessel model, compared with measured aortic pressure.

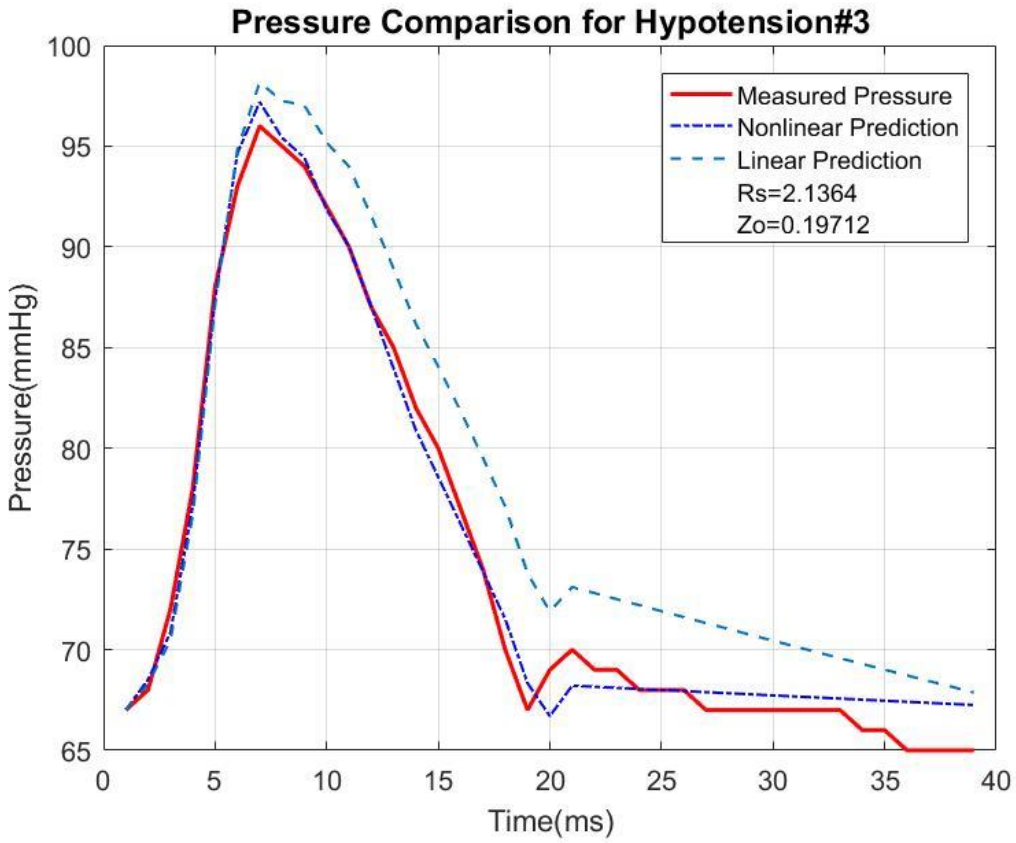

Fig 4.9: Aortic pressure approximation for vasodilation #3. Pressure of vasodilation case #3 predicted by linear Windkessel model, nonlinear Windkessel model, compared with measured aortic pressure.

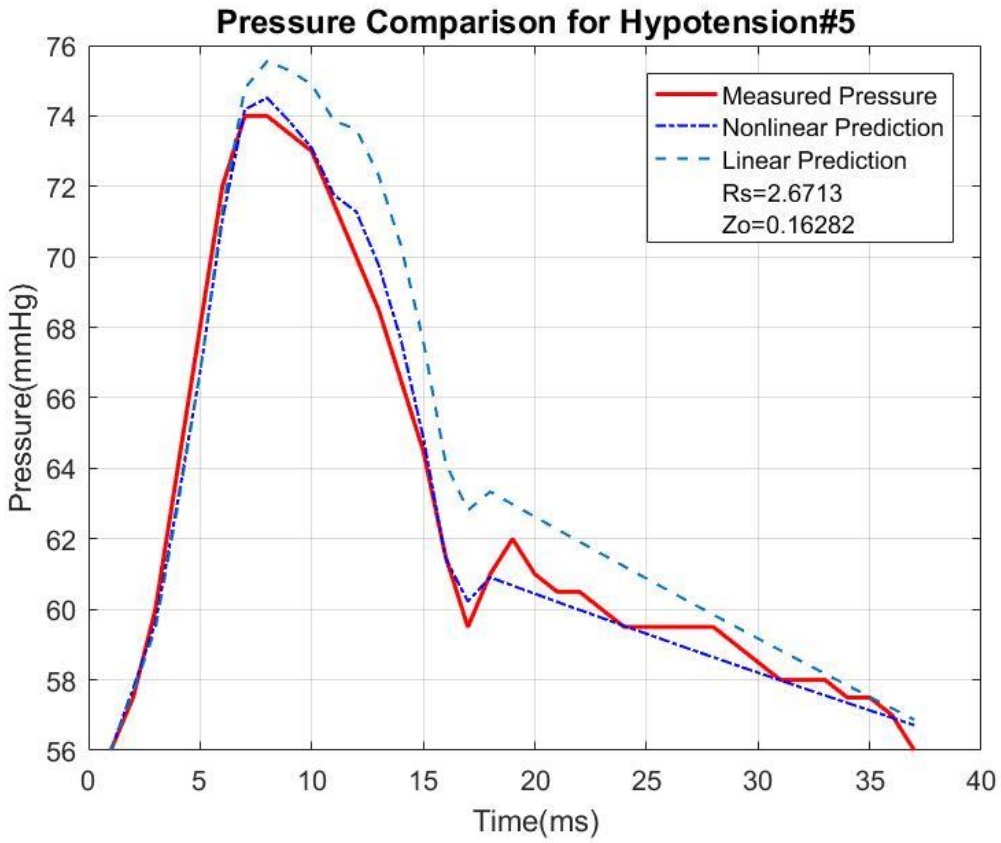

Fig 4.10: Aortic pressure approximation for vasodilation #5. Pressure of vasodilation case #5 predicted by linear Windkessel model, nonlinear Windkessel model, compared with measured aortic pressure.

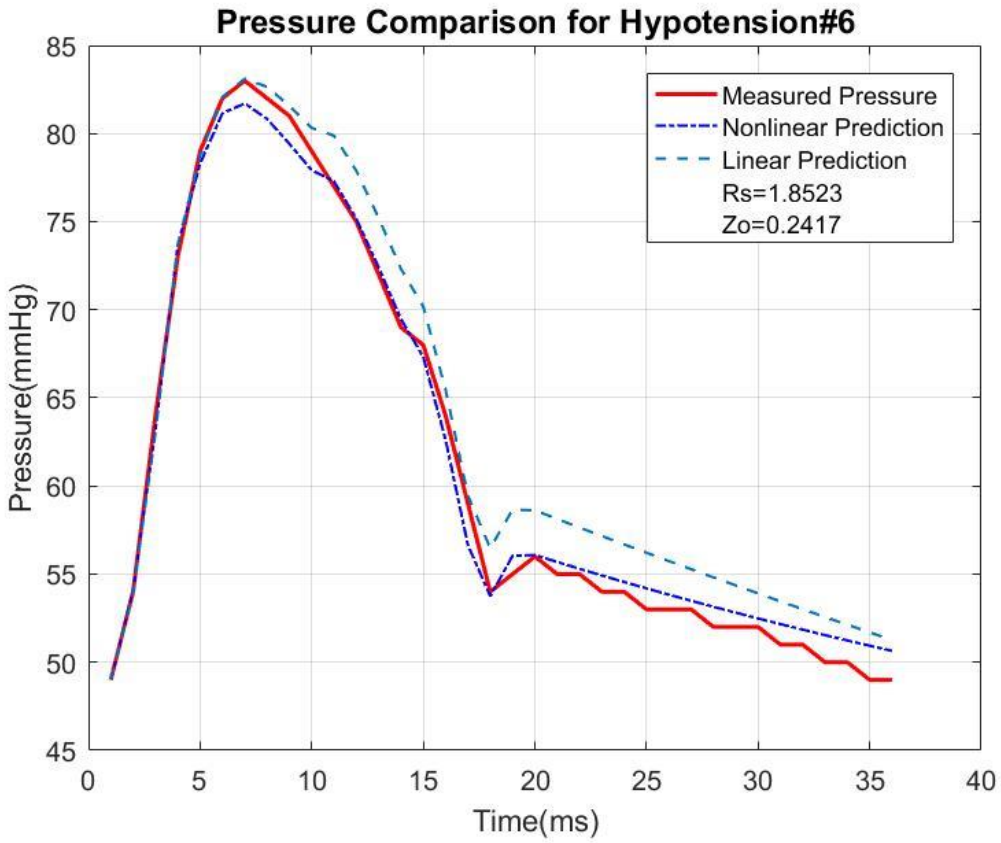

Fig 4.11: Aortic pressure approximation for vasodilation #6. Pressure of vasodilation case #6 predicted by linear Windkessel model, nonlinear Windkessel model, compared with measured aortic pressure.

In most cases, nonlinear modeling has dominant advantages over the linear one. Both predictions are fairly accurate in early systolic stage, whereas nonlinear model generates closer estimations from end-systolic to diastolic period. This outcome indicates that incorporating a continuously varying compliance can significantly improve the reliability of three-element Windkessel model in predicting hemodynamic activities. This aspect become much clearer in the following section.

4.2 Pressure-Compliance Loop

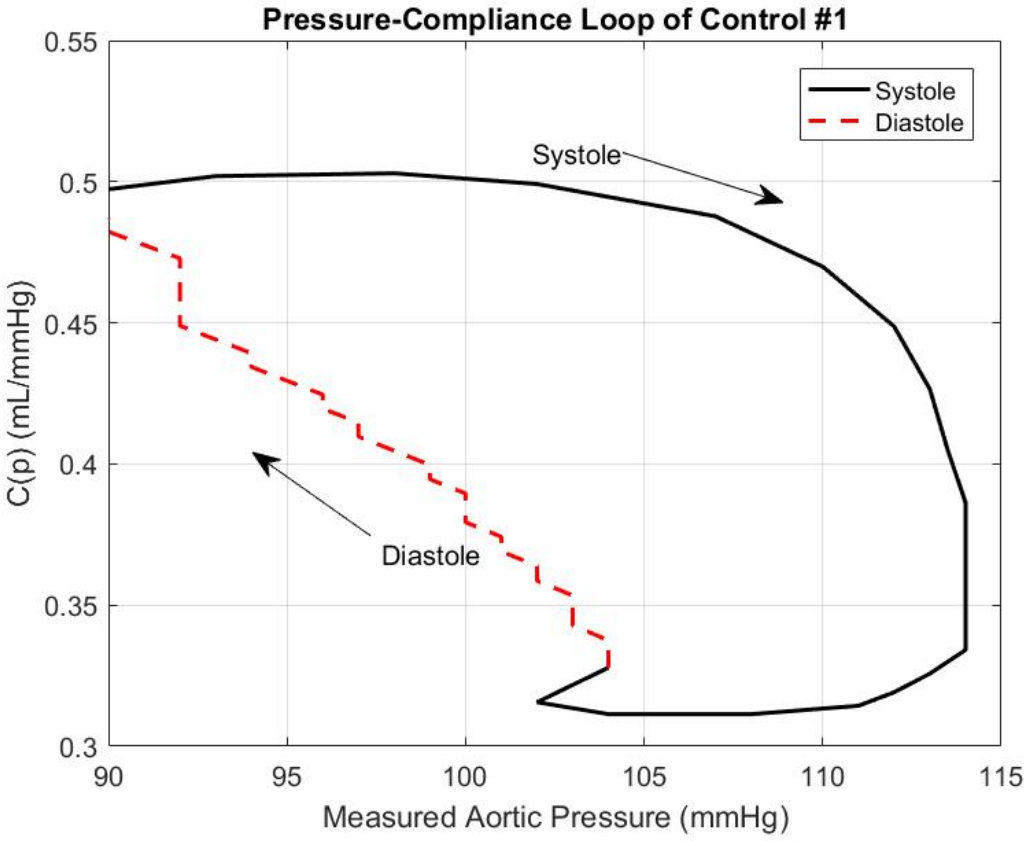

Fig 4.12: Pressure-Compliance loop of normal case #1, implying a dynamic relationship between pressure change and vascular stiffness (1/C(P)).

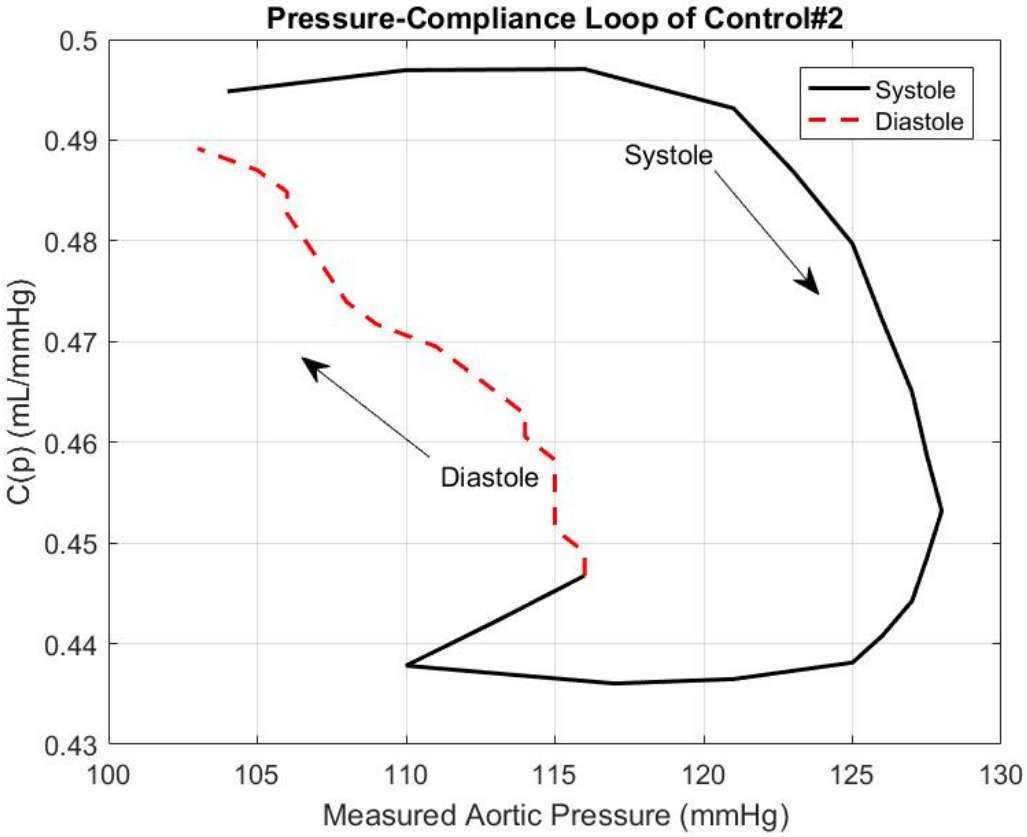

Fig 4.13: Pressure-Compliance loop of normal case #2, implying a dynamic relationship between pressure change and vascular stiffness(1/C(P)).

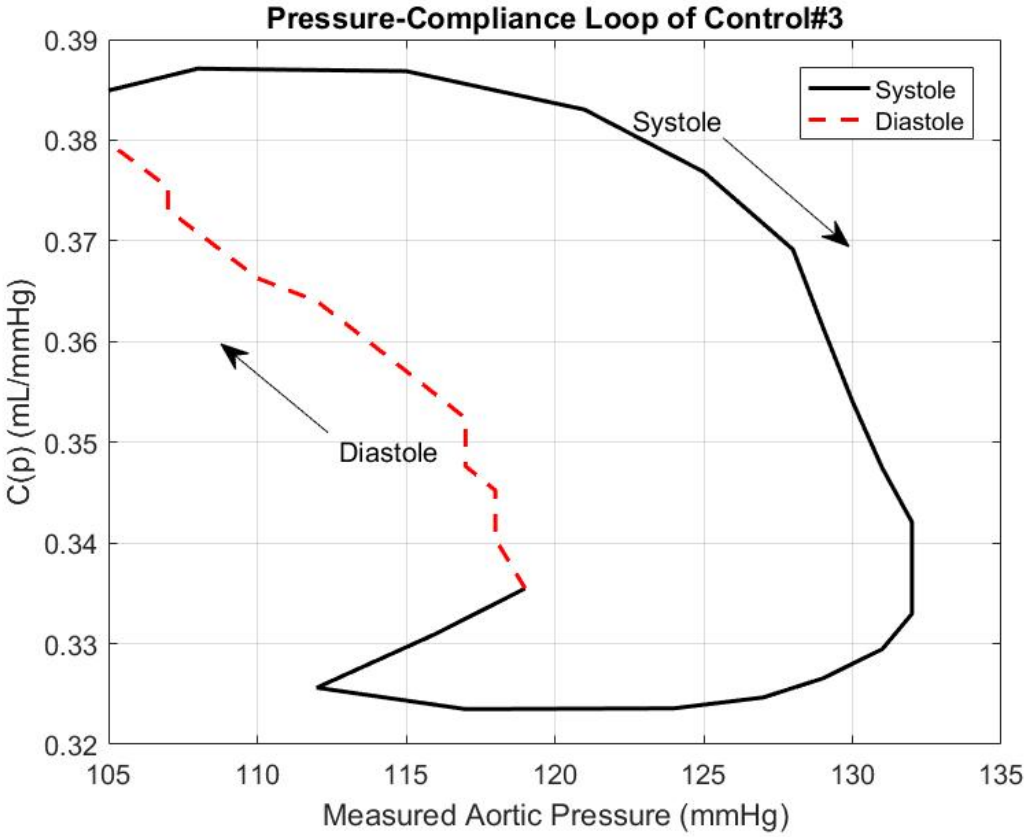

Fig 4.14: Pressure-Compliance loop of normal case #3, implying a dynamic relationship between pressure change and vascular stiffness(1/C(P)).

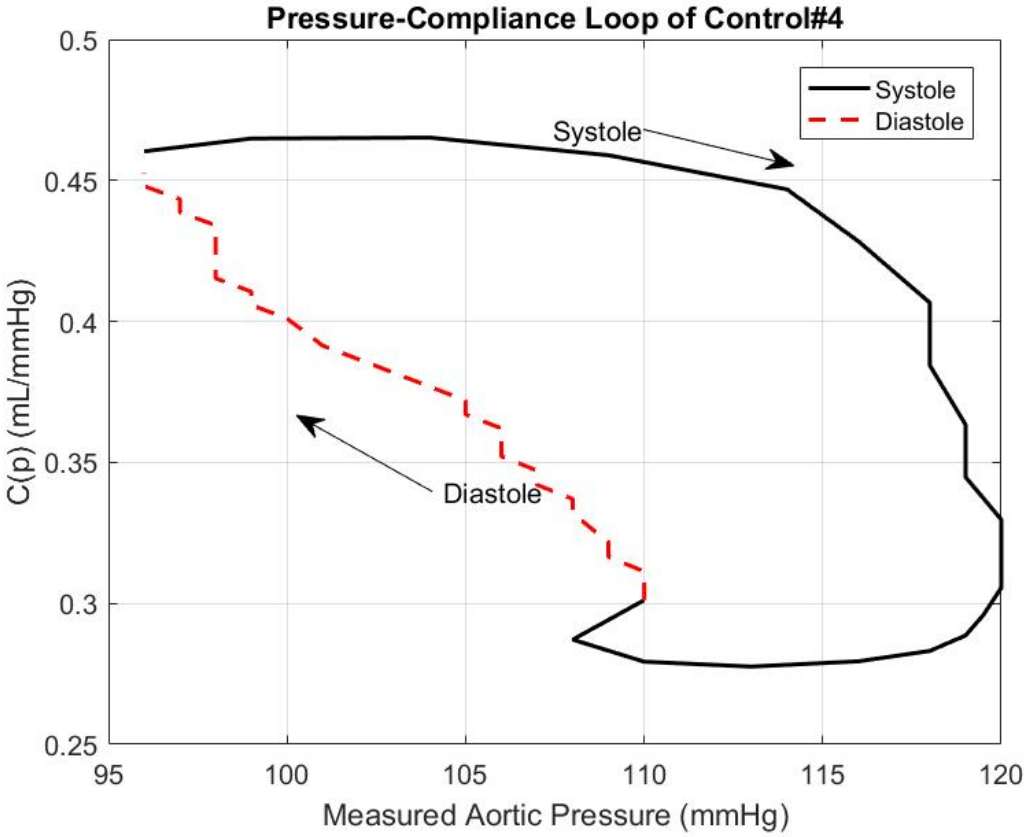

Fig 4.15: Pressure-Compliance loop of normal case #4, implying a dynamic relationship between pressure change and vascular stiffness(1/C(P)).

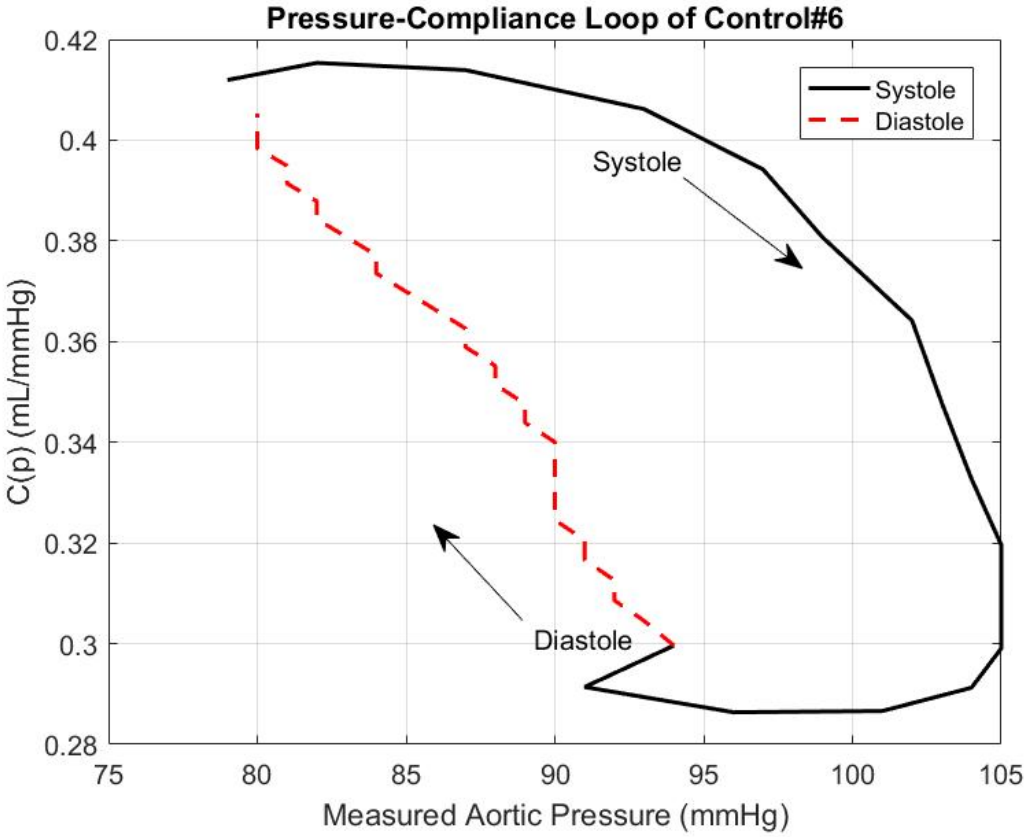

Fig 4.16: Pressure-Compliance loop of normal case #6, implying a dynamic relationship between pressure change and vascular stiffness(1/C(P)).

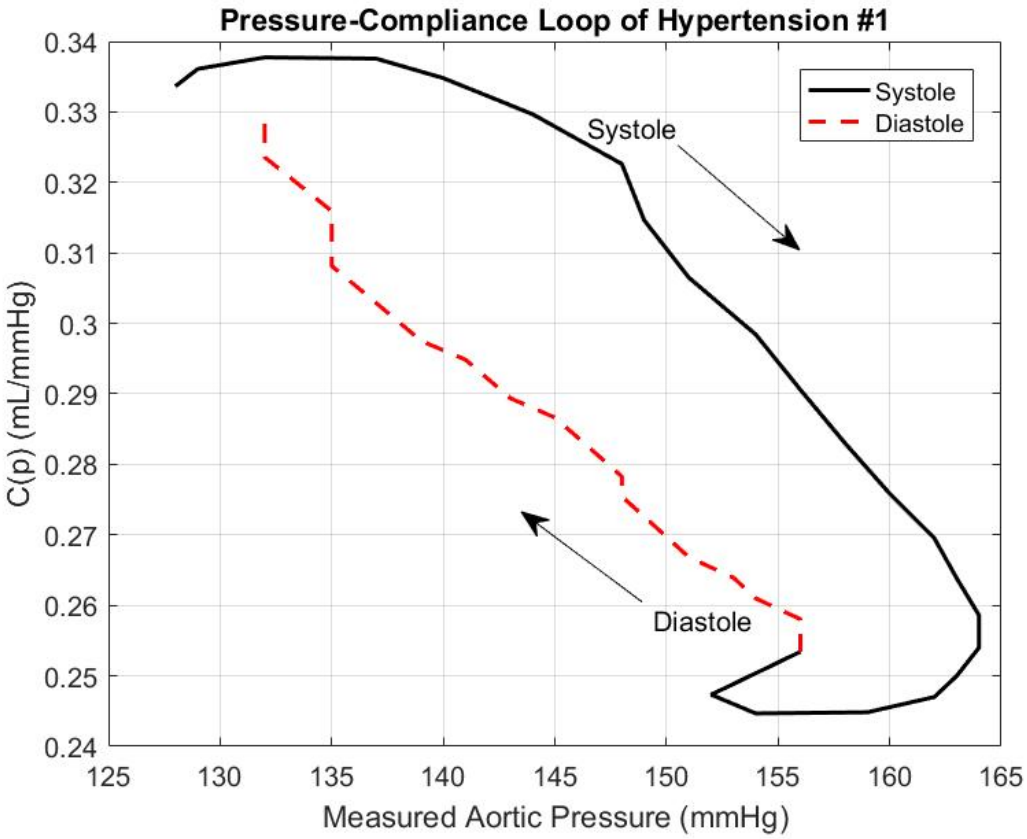

Fig 4.17: Pressure-Compliance loop of hypertension case #1, implying a dynamic relationship between pressure change and vascular stiffness(1/C(P)).

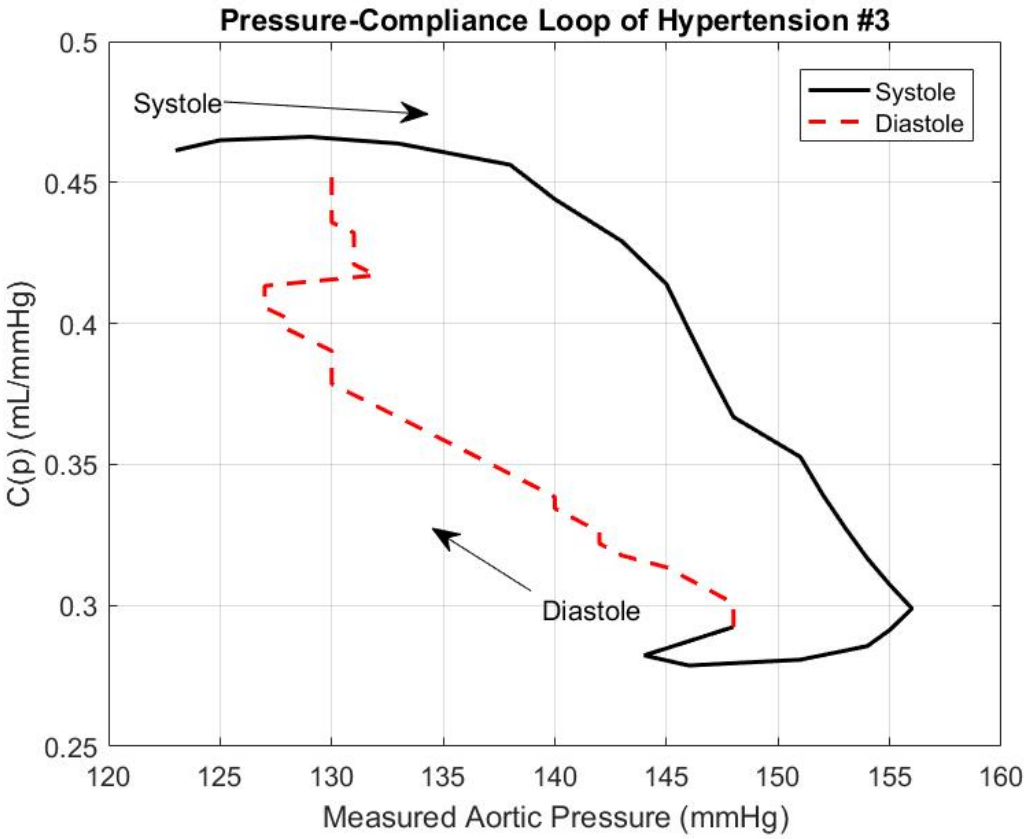

Fig 4.18: Pressure-Compliance loop of hypertension case #3, implying a dynamic relationship between pressure change and vascular stiffness(1/C(P)).

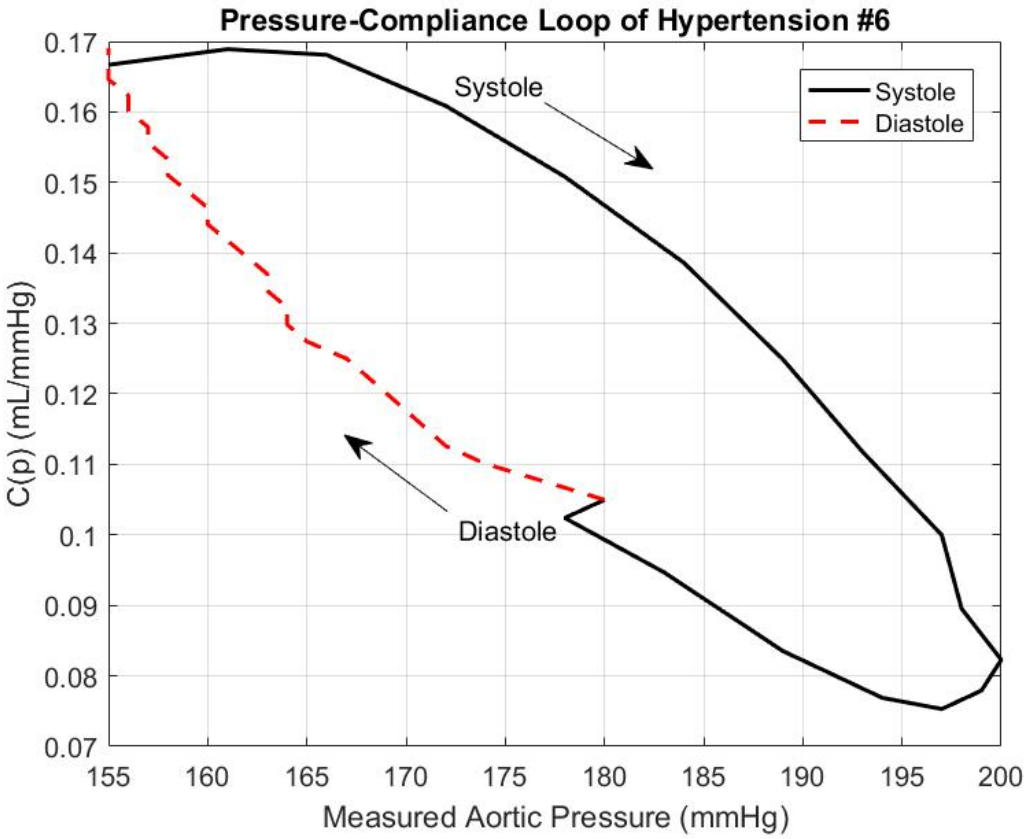

Fig 4.19: Pressure-Compliance loop of hypertension case #6, implying a dynamic relationship between pressure change and vascular stiffness(1/C(P)).

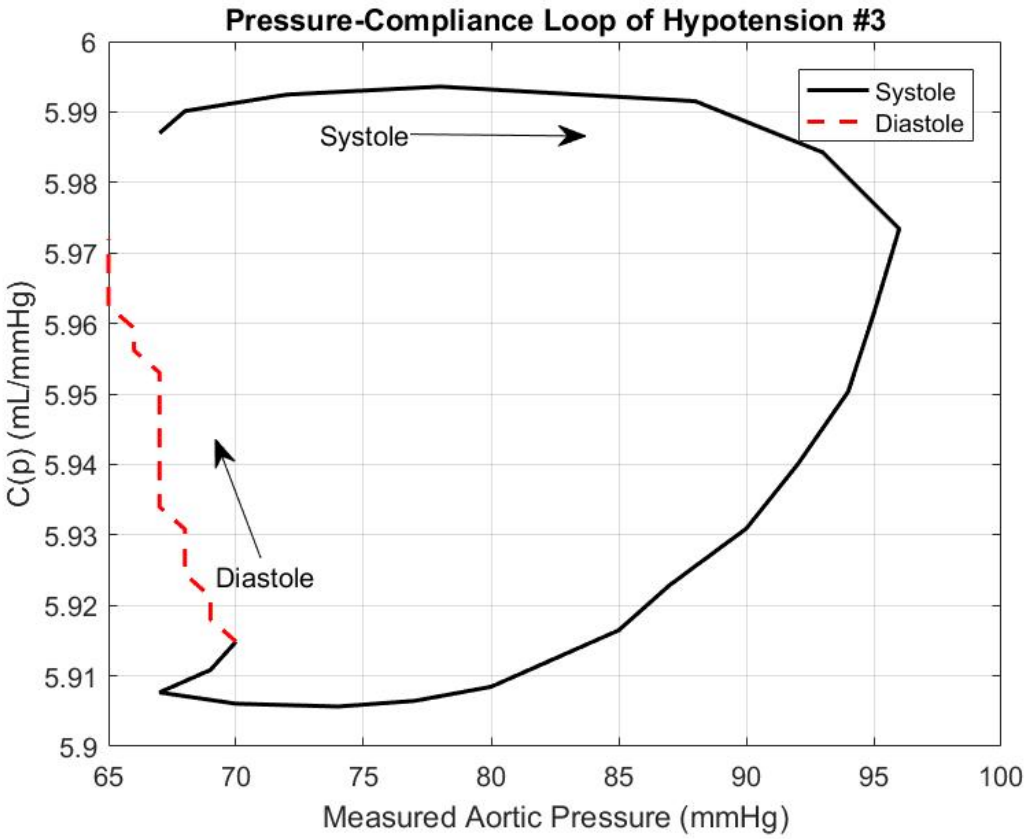

Fig 4.20: Pressure-Compliance loop of vasodilation case #3, implying a dynamic relationship between pressure change and vascular stiffness(1/C(P)).

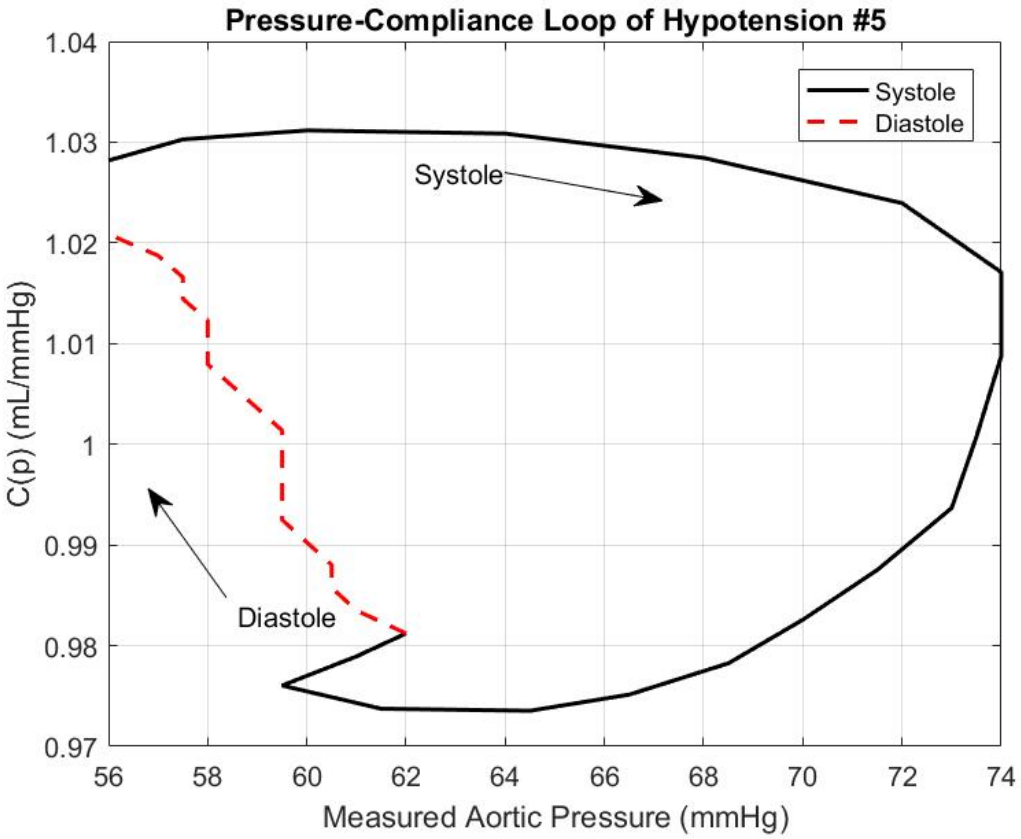

Fig 4.21: Pressure-Compliance loop of vasodilation case #5, implying a dynamic relationship between pressure change and vascular stiffness(1/C(P)).

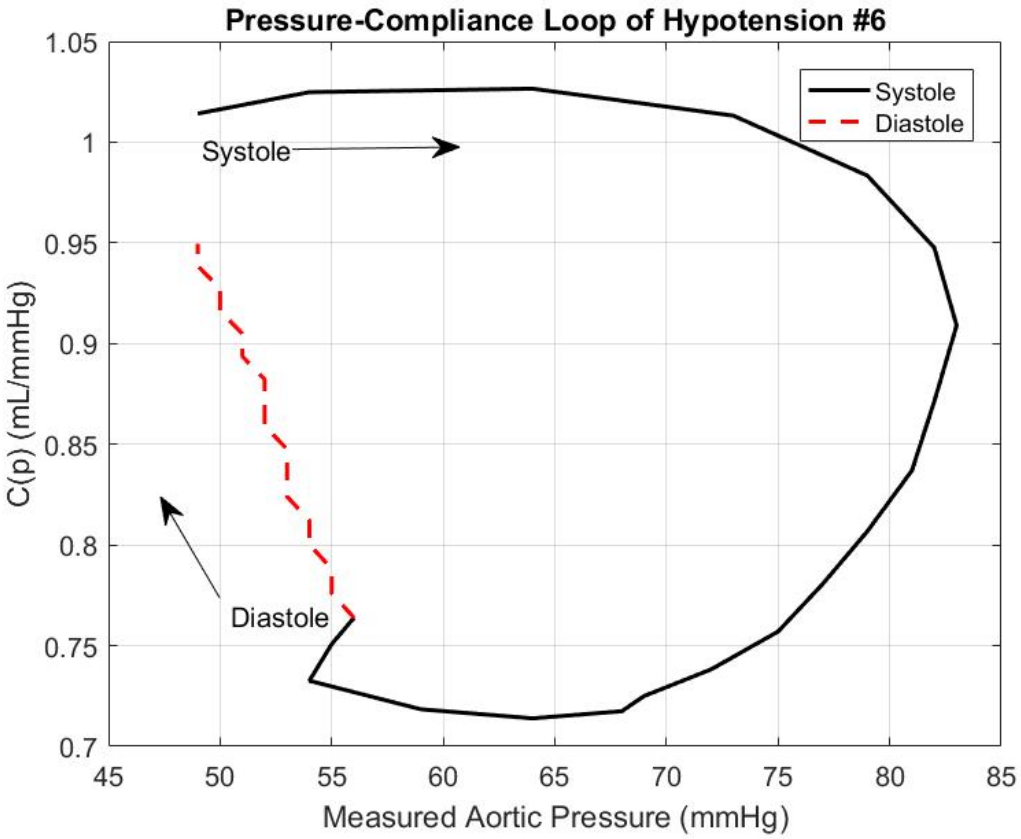

Fig 4.22: Pressure-Compliance loop of vasodilation case #6, implying a dynamic relationship between pressure change and vascular stiffness(1/C(P)).

Arrows were used to directionally indicate the compliance change along with pressure increasing and declining. Generally, compliance starts decreasing when ejection during contraction of the heart begins and as aorta becomes stiffer with increasing aortic pressure. This reaches a maximum at end of systole at the closure of the aortic valve and aortic flow ceases. In case of hypertension (vasoconstriction), the compliance is reduced with a very steep slope during the beginning of ejection, then increases throughout the diastole when, as expected, aortic pressure falls. The compliance will reach to its peak

value at end of diastole and start over for next cardiac cycle. Dissimilarly, under the circumstances of vasodilation, the compliance falls slowly during early contraction with a flattened slope. The loops in these cases are much greater, signaling greater opening of the arterial lumen area as compared to those in the hypertensive conditions. This aspect will be discussed in the following chapter.

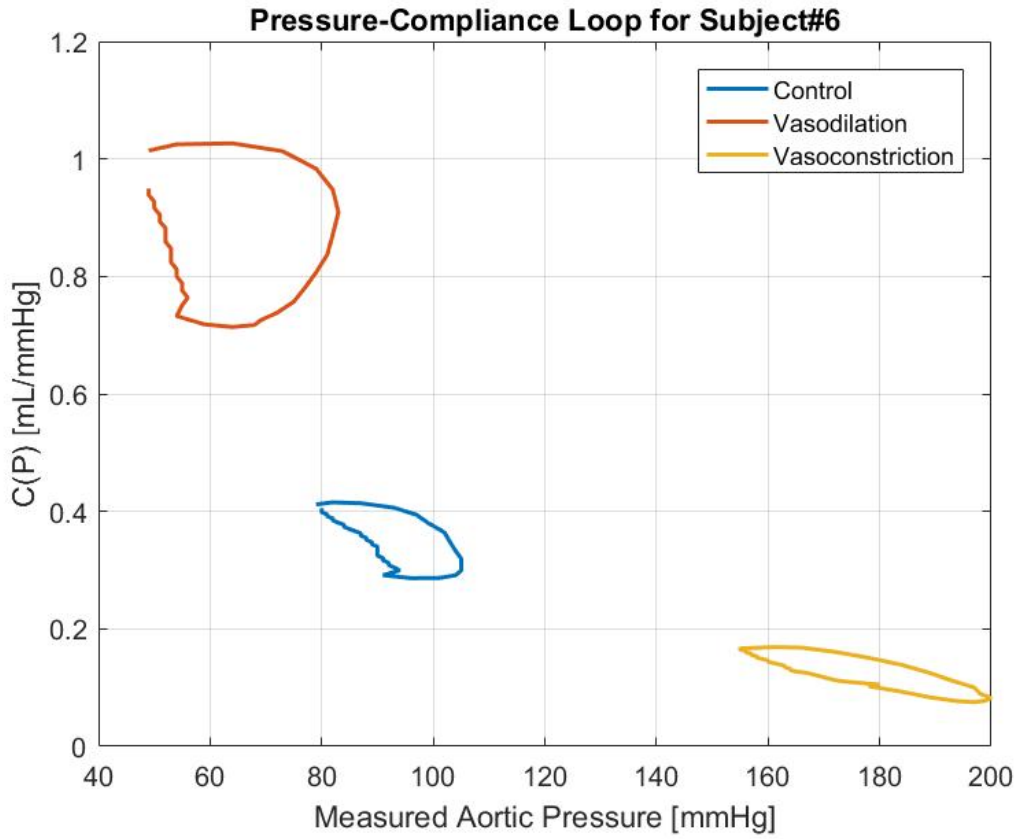

Fig 4.23: Comparison of compliance-pressure loops over a cardiac cycle. The data was from one subject under normal, vasodilated (vasodilator treated) and vasoconstricted (hypertension) conditions.

Fig 4.23 provides a comparison of the pressure-compliance loops under all three studied conditions, i.e. normal control, hypertension and vasodilator-treated. It is readily recognized that higher compliance exists in vasodilation, which complies with the fact that nitroprusside relaxes vascular smooth muscles and therefore enhances compliance. Likewise, it is explainable that hypertensive loop has lowest compliance among three conditions. Under vasoconstriction, vessels become stiffer, meaning a small change in flow volume will cause a large rise in pressure.

Moreover, unlike a compliance calculated from linear Windkessel or stroke volume method that retains unchanged over time, this pressure-dependent compliance obtains us a more comprehensive insight into vascular systems during the entire contraction. A comparison of compliances derived from linear Windkessel (Ct), stroke volume method (Cv) and nonlinear Windkessel (C(P)) is shown in Table4.1. It is worth noted that first two methods usually underestimate the compliance of vessels, providing a potent evidence that C(P) has significant contribution in aortic pressure predictions.

Table 4.1 Comparison of linear and nonlinear calculations of compliance with related parameters. MTX= methoxamine induced vasoconstriction. NTP=nitroprusside induced vasodilation

Dataset	**Ct [mL/ mmHg]**	**Cv [mL/ mmHg]**	**C(P) max [mL/ mmHg]**	**C(P) min [mL/ mmHg]**	**HR [beats/ min]**	**Ps mmHg**	**Pd mmHg**	**Rs mmHg ·s/mL**
Control Group								
#1	0.3667	0.3750	0.5030	0.3114	115.38	114	90	5.8427
#2	0.3242	0.3560	0.4971	0.4360	157.89	128	103	4.9303
#3	0.3129	0.3519	0.3871	0.3235	153.85	132	105	4.8511
#4	0.3468	0.3583	0.4652	0.2776	117.65	120	96	6.3541
#6	0.3718	0.3354	0.4153	0.2864	133.33	105	80	4.6697
Mean ± SD	0.3445 ± 0.0258	0.3553 ± 0.0142	0.4535 ± 0.0509	0.327 ± 0.0637				
MTX Group								
#1	0.3091	0.3883	0.3377	0.2447	120	164	120	5.2296

#3	0.4527	0.3873	0.4662	0.2787	95.24	156	130	6.8130
#6	0.1284	0.1218	0.169	0.0753	133.33	200	155	14.0675
Mean ± ***SD***	0.2967 ± 0.1625	0.2991 ± 0.1536	0.3243 ± 0.1491	0.1996 ± 0.109				
NTP Group								
#3	1.1369	0.4373	5.9936	5.9057	153.84	96	65	2.1364
#5	0.6620	0.4817	1.0312	0.9735	162.16	74	56	2.6713
#6	0.6469	0.3506	1.0265	0.7139	166.67	83	49	1.8523
Mean ± ***SD***	0.8153 ± 0.2786	0.4232 ± 0.0667	2.6838 ± 2.8664	2.531 ± 2.9254				

Chapter 5 Discussion and Suggestions for Future Research

5.1 Advantages of the Compliance-Pressure Loop based on the Nonlinear Model of the Arterial System.

Modeling facilitates the exploration of physiological information from limited sources. Only simultaneously measured pressure and flow are required for the Windkessel model in providing several crucial characteristics of the arterial system. Although lumped model failed to predict propagating pressure and flow compared with distributed model, it provides a simplified approach to obtaining gross feature of arterial system function (Noordergraaf, 1978; Li, 1987; Li, 2000).

The traditional three-element Windkessel model with a constant arterial system compliance assumes the elastic modulus remains unchanged during the entire ejection. This formulation has been widely used for years despite that compliance is known to vary continuously with pressure change.

Recently, nonlinear three-element Windkessel model has been extensively applied to simulated and experimental data. The feasibility of this method has also been identified effective in different circulatory conditions (Cappello,1995). In the present study, a dynamic association between pressure and vascular compliance has been established with the inclusion of a pressure-dependent arterial compliance element (C(P)) replacing the constant compliance C in the classic three element Windkessel model. As a result, the nonlinear compliance estimated from this modified model expressed an excellent discernibility during each stage of systole under varied vasoactive states. In addition, improvement is made on the extension of the previous approach based on the root mean

square error (RMSE) method. This approach has shown to fit the nonlinear model predicted pressure waveform better in vasodilation and vasoconstriction cases (Table 5.1).

The concept of pressure-compliance loop provides a detailed interpretation of the structural properties of arterial wall interacting with underlying pulsatile pressure-flow relationship. One of the marked observations is that during systole and diastole, pressure could reach the same value while compliance differed. This result highlights a speculation, which was often omitted, that mechanical properties of vessels have changed from systole to diastole. In other words, the vascular elastance varies throughout the cardiac cycle even under same pressure level. Also, it reminds us that reflected pressure and forward pressure play an important role in determining the vascular load to the contracting heart. This aspect is further discussed in a later section.

Last but not least, the compliance loop shapes change drastically in hypertension cases, representing a compressed and stiff vessel. Conversely, the compliance loop of hypotension is more rounded with observably larger underlying area. Therefore, the loops can be utilized as a potential indicator of medications efficacy on antihypertensive drugs and classify the severity of hypertension.

Table 5.1: Comparison of Root Mean Square Errors (RMSE). Results are generated from the comparison between measured aortic pressure and linear Windkessel model, nonlinear Li Model, respectively.

Control Group	**Linear Windkessel**	**Nonlinear Li Model**
#1	2.2320	1.6326
#2	3.5777	2.0202
#3	2.3325	1.8890
#4	1.9931	1.4716
#6	0.7943	0.8626
MTX Group		
#1	1.5621	1.8115
#3	3.2607	2.6919
#6	5.2911	3.2642
NTP Group		
#3	3.6283	1.2003
#5	1.7611	0.6262
#6	2.2560	1.0179

5.2 Drug Effects on Arterial Compliance

Numerous studies have been conducted towards the effect of different drugs on reducing stiffness of central aorta (increasing arterial compliance), in order to eventually select optimal treatment for hypertension as well as other related cardiovascular diseases. For instance, LR-90, a glycation inhibitor has been identified as a significant factor that

protects patient from aortic stiffening induced by diabetes or the cardiac hypertrophy. (Satheesan et al, 2014). Following administration of LR-90, a considerable improvement of hemodynamic parameters was quantified, and these mechanical alterations led an early back flow from the peripheries. An addition of niacin with a statin in treating type 2 diabetic patients exhibited amelioration on small artery vasodilatory function and increase in compliance (Hamilton et al, 2010). Allopurinol was also claimed to have effect on facilitating aortic compliance independently of thiazide-based antihypertensive therapy while significantly dependent on initial pulse wave velocity in the aorta (Kostka-Jeziorny et al., 2011). Other therapies such as amlodipine and bisoprolol (Iekh et al., 2014), fixed perindopril A/Amlodipine combination (Glezer et al., 2015) were proved to have effect on blood pressure mediation by increase arterial compliance.

It is clear that antihypertensive therapies increasingly focus on ameliorating mechanical properties especially compliance of arteries, for a better therapeutic outcome. The compliance-pressure loop can be better utilized as a representation for assessing treatment efficacy. Computing compliance-pressure loops under pre and post treatment will provide the clinicians the visualization and an objective conclusion of whether the drug unloads the heart adequately.

5.3 Suggestions for Future Study: Consideration of the Effect of Wave Reflections on Arterial Compliance

Pressure and flow can be resolved into their respective forward and backward components during each cardiac cycle. (Newman et al., 1979; Westerhof et al., 1972; Womersley 1958; Li, 1986; Nichols et al., 2011). Increase in arterial pressure pulse

wave reflection will elevate central aortic blood pressure and thereby placing a burden as cardiac afterload. Increased pulse wave reflection has been shown as a risk factor of cardiovascular diseases along with aging and hypertension (Van De Vosse et al., 2011; Manisty et al., 2010; Latham et al., 1985; Laskey et al., 1987; Matsui et al., 2004). Meanwhile, pressure and flosw damping are attenuated by decline of arterial distensibility, where wave reflection yields early systole and augments peak systolic pressure as well as pulse pressure (O'Rourke et al., 1990; Stergiopulos et al., 1998). In this regards, arterial compliance is tightly associated with wave reflections and the latter can be considered as a viable index in understanding and predicting cardiovascular function.

Decreased arterial compliance has been shown to be associated with increased wave reflections, due to increased impedance to blood flow (Li, 2000, 2004) In the extended study of this thesis, forward and backward pressure components were computed under normal and hypertensive conditions. Substituting equation (1.3) and (1.4) with previously predicted aortic pressure and characteristic impedance, these two pressure waveforms were generated. Compliance of control case is 0.2864 to 0.4153 mL/mmHg, compared to the one of hypertension case that is 0.0753 to 0.169 mL/mmHg (Table 4.1). It is clearly implied from Fig 5.1 and Fig 5.2 that reflected wave greatly escalated with respect to the forward wave (i.e., increased reflection coefficient increases), in correspondence with a reduction in arterial compliance.

In the future study, the effect of wave reflections on arterial compliance should be investigated, with a goal to quantitatively analyze their relationship during normal control, hypertension and drug therapy.

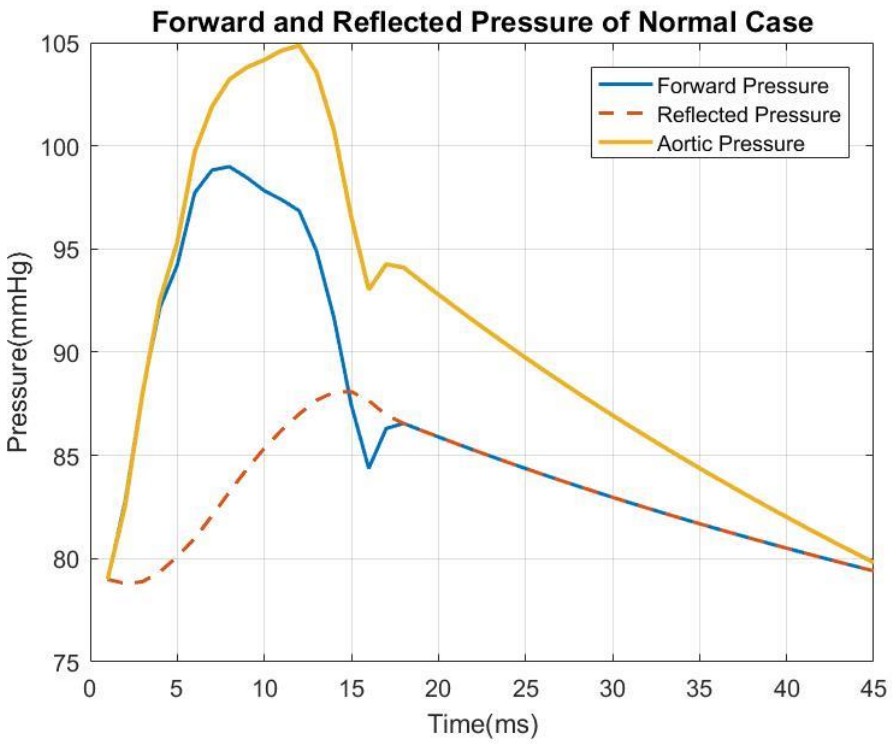

Fig 5.1: Central blood pressure resolved into forward and reflected pressure under normal condition.

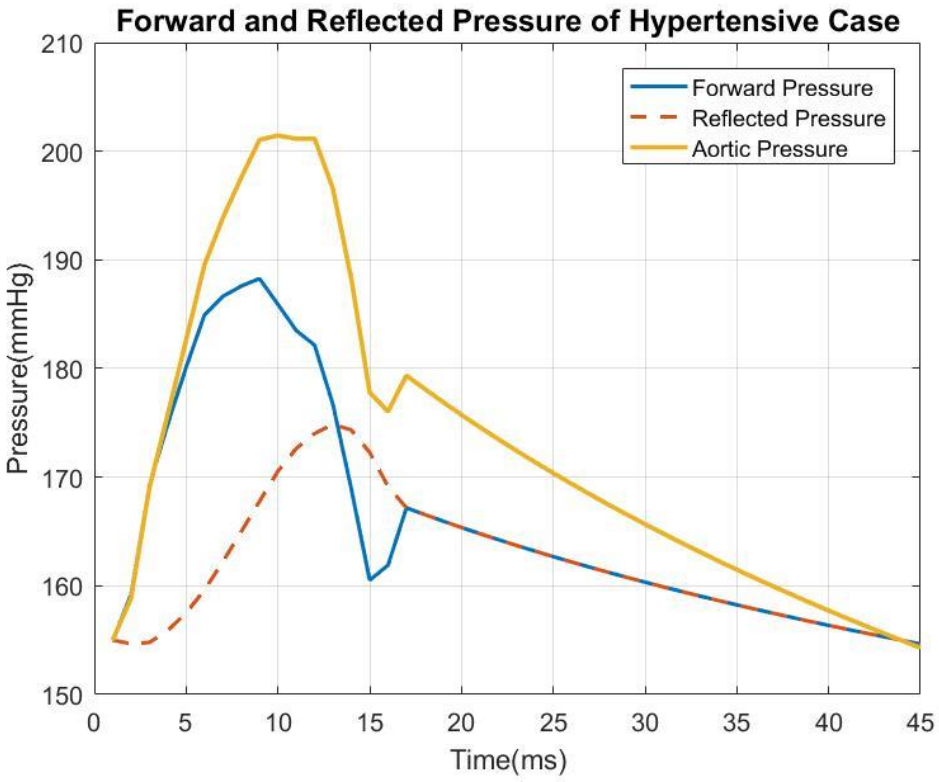

Fig 5.2: Central blood pressure resolved into forward and reflected pressure under hypertensive condition.

Reference

[1] Kannel, W. B. (1996). Blood pressure as a cardiovascular risk factor: prevention and treatment. *Jama*, *275*(20), 1571-1576.

[2] Pickering, T. G. (2006). New ways of measuring blood pressure. *American journal of hypertension*, *19*(10), 988-990.

[3] Penaz, J. (1973). Photoelectric measurement of blood pressure, volume and flow in the finger. *In Digest 10th International Conference on Medical and Biological Engineering, p. 104. Dresden.*

[4] Ogedegbe, G., & Pickering, T. (2010). Principles and techniques of blood pressure measurement. *Cardiology clinics*, *28*(4), 571-586.

[5] Agabiti-Rosei, E., Mancia, G., O'rourke, M. F., Roman, M. J., Safar, M. E., Smulyan, H., ... & Vlachopoulos, C. (2007). Central blood pressure measurements and antihypertensive therapy: a consensus document. *Hypertension*, *50*(1), 154-160.

[6] Nichols, W.W., O'Rourke, M.F., McDonald, D.A. (2005). *McDonald's blood flow in arteries: theoretical, experimental and clinical principles*. Paris, France, Oxford University Press.

[7] Safar, M., & O'Rourke, M. F. (2006). *Arterial stiffness in hypertension* (Vol. 23). Elsevier Health Sciences.

[8] Laurent, S., Boutouyrie, P., Asmar, R., Gautier, I., Laloux, B., Guize, L., ... & Benetos, A. (2001). Aortic stiffness is an independent predictor of all-cause and cardiovascular mortality in hypertensive patients. *Hypertension*, *37*(5), 1236-1241.

[9] Vlachopoulos, C., Aznaouridis, K., & Stefanadis, C. (2010). Prediction of cardiovascular events and all-cause mortality with arterial stiffness: a systematic review and meta-analysis. *Journal of the American College of Cardiology*, *55*(13), 1318-1327.

[10] Mitchell, G. F., Hwang, S. J., Vasan, R. S., Larson, M. G., Pencina, M. J., Hamburg, N. M., ... & Benjamin, E. J. (2010). Arterial stiffness and cardiovascular events: the Framingham Heart Study. *Circulation*, *121*(4), 505-511.

[11] Safar, M. E. (2001). Systolic blood pressure, pulse pressure and arterial stiffness as cardiovascular risk factors. *Current opinion in nephrology and hypertension*, *10*(2), 257-261.

[12] Frank, O. (1990). The basic shape of the arterial pulse. First treatise: mathematical analysis. *Journal of molecular and cellular cardiology*, *22*(3), 255-277.

[13] Dujardin, J. P. L., & Stone, D. N. (1981). Characteristic impedance of the proximal aorta determined in the time and frequency domain: a comparison. *Medical and Biological Engineering and Computing*, *19*(5), 565-568.

[14] Li, J. K.J. (2004). Dynamics of the vascular system. *World Scientific*, Singapore.

[15] Li, J. K.J. (2000). The Arterial Circulation: Physical Principles and Clinical Applications. *Springer, New York.*

[16] Liu, Z. R., Ting, C. T., Zhu, S. X., & Yin, F. C. (1989). Aortic compliance in human hypertension. *Hypertension*, *14*(2), 129-136.

[17] Wang, J. J., Liu, S. H., Kao, T., Hu, W. C., & Liu, C. P. (2006). Noninvasive determination of arterial pressure-dependent compliance in young subjects using an arterial tonometer. *Biomedical Engineering: Applications, Basis and Communications*, *18*(03), 111-118.

[18] Li, J. K., Cui, T., & Drzewiecki, G. M. (1990). A nonlinear model of the arterial system incorporating a pressure-dependent compliance. *IEEE Transactions on Biomedical Engineering*, *37*(7), 673-678.

[19] Shirai, K., Utino, J., Otsuka, K., & Takata, M. (2006). A novel blood pressure-independent arterial wall stiffness parameter; cardio-ankle vascular index (CAVI). *Journal of atherosclerosis and thrombosis*, *13*(2), 101-107.

[20] Murphy, S. L., Xu, J., Kochanek, K. D., Curtin, S. C., & Arias, E. (2017). Deaths: final data for 2015.

[21] Segers, P., Verdonck, P., Deryck, Y., Brimioulle, S., Naeije, R., Carlier, S., & Stergiopulos, N. (1999). Pulse pressure method and the area method for the estimation of total arterial compliance in dogs: sensitivity to wave reflection intensity. *Annals of biomedical engineering*, *27*(4), 480-485.

[22] Li, J. K., & Zhu, Y. (1994). Arterial compliance and its pressure dependence in hypertension and vasodilation. *Angiology*, *45*(2), 113-117.

[23] Li, J. K. (1986). Time domain resolution of forward and reflected waves in the aorta. *IEEE transactions on biomedical engineering*, (8), 783-785.

[24] Noordergraaf, A. (1978). Circulatory system dynamics. *New York: Academic*.

[25] Li, J. K. (1987). Arterial System Dynamics. *New York: New York Univ*.

[26] Cappello, A., Gnudi, G., & Lamberti, C. (1995). Identification of the three-element windkessel model incorporating a pressure-dependent compliance. *Annals of biomedical engineering*, *23*(2), 164-177.

[27] Satheesan, S., Figarola, J. L., Dabbs, T., Rahbar, S., & Ermel, R. (2014). Effects of a new advanced glycation inhibitor, LR-90, on mitigating arterial stiffening and improving arterial elasticity and compliance in a diabetic rat model: aortic impedance analysis. *British journal of pharmacology*, *171*(12), 3103-3114.

[28] Hamilton, S. J., Chew, G. T., Davis, T. M., & Watts, G. F. (2010). Niacin improves small artery vasodilatory function and compliance in statin-treated type 2 diabetic patients. *Diabetes and Vascular Disease Research*, *7*(4), 296-299.

[29] Kaya, M., Balasubramanian, V., Patel, A., Ge, Y., & Li, J. K. (2018). A novel compliance-pressure loop approach to quantify arterial compliance in systole and in diastole. *Computers in biology and medicine*.

[30] Kostka-Jeziorny, K., Uruski, P., & Tykarski, A. (2011). Effect of allopurinol on blood pressure and aortic compliance in hypertensive patients. *Blood pressure*, *20*(2), 104-110.

[31] Zaremba, I., Zaremba-Fedchyshyn, O. V., Virna, M. M., Bula, M. S., & Zaremba, O. V. (2014). Amlodipine and bisoprolol application in patients with arterial hypertension. *Wiadomosci lekarskie (Warsaw, Poland: 1960)*, *67*(2 Pt 2), 326-327.

[32] Glezer, O. B. O. P. P. (2015). The Use of Fixed Perindopril A/Amlodipine Combination Provides High Compliance to Therapy, Effective and Safe Arterial Pressure Lowering in Patients with Previous Inefferctive Therapy. The POTENTIAL Program. *Kardiologiia*, *55*(12), 17.

[33] Newman, D. L., Greenwald, S. E., & Bowden, N. L. R. (1979). An in vivo study of the total occlusion method for the analysis of forward and backward pressure waves. *Cardiovascular research*, *13*(10), 595-600.

[34] Westerhof, N., Sipkema, P., Bos, G. V. D., & Elzinga, G. (1972). Forward and backward waves in the arterial system. *Cardiovascular research*, *6*(6), 648-656.

[35] Womersley, J. R. (1958). Oscillatory flow in arteries. II: The reflection of the pulse wave at junctions and rigid inserts in the arterial system. *Physics in Medicine & Biology*, *2*(4), 313.

[36] Nichols, W.W., O'Rourke, M.F. (2011). McDonald's Blood Flow in Arteries: Theoretical Experimental and Clinical Principles. *USA, FL, Boca Raton:CRC Press*.

[37] Van de Vosse, F. N., & Stergiopulos, N. (2011). Pulse wave propagation in the arterial tree. *Annual Review of Fluid Mechanics*, *43*, 467-499.

[38] Manisty, C., Mayet, J., Tapp, R. J., Parker, K. H., Sever, P., Poulter, N. H., ... & ASCOT Investigators. (2010). Wave reflection predicts cardiovascular events in hypertensive individuals independent of blood pressure and other cardiovascular risk factors: an ASCOT (Anglo-Scandinavian Cardiac Outcome Trial) substudy. *Journal of the American College of Cardiology*, *56*(1), 24-30.

[39] Latham, R. D., Westerhof, N., Sipkema, P., Rubal, B. J., Reuderink, P., & Murgo, J. P. (1985). Regional wave travel and reflections along the human aorta: a study with six simultaneous micromanometric pressures. *Circulation*, *72*(6), 1257-1269.

[40] Laskey, W. K., & Kussmaul, W. G. (1987). Arterial wave reflection in heart failure. *Circulation*, *75*(4), 711-722.

[41] Matsui, Y., Kario, K., Ishikawa, J., Eguchi, K., Hoshide, S., & Shimada, K. (2004). Reproducibility of arterial stiffness indices (pulse wave velocity and augmentation index) simultaneously assessed by automated pulse wave analysis and their associated risk factors in essential hypertensive patients. *Hypertension Research*, *27*(11), 851-857.

[42] O'rourke, M. (1990). Arterial stiffness, systolic blood pressure, and logical treatment of arterial hypertension. *Hypertension*, *15*(4), 339-347.

[43] Stergiopulos, N., & Westerhof, N. (1998). Determinants of pulse pressure. *Hypertension*, *32*(3), 556-559.

[44] American Heart Association News. (2017, November 13). *Nearly half of U.S. adults could now be classified with high blood pressure, under new definitions*. Retrieved from https://www.heart.org